Alma Mater Studiorum – Università di Bologna

DOTTORATO DI RICERCA IN
INGEGNERIA CIVILE, CHIMICA, AMBIENTALE
E DEI MATERIALI

XIX Ciclo

Settore Concorsuale di afferenza: 09/D1
Settore Scientifico disciplinare: Scienza e Tecnologia dei Materiali (ING-IND/22)

Sustainable waste-based materials for conservation of built environment

Presentata da:

Ing. Parsa Pahlavan

Coordinatore Dottorato
Prof. Luca Vittuari

Relatore
Prof. Maria Chiara Bignozzi

Correlatori

Dr. Stefania Manzi
Dr. Antonio Sansonetti

Esame finale anno 2017

از دی که گذشت هیچ از و یاد مکن
فردا که نیامده ست فریاد مکن
بر نامده و گذشته بنیاد مکن
حالی خوش باش و عمر برباد مکن

Non ricordare il giorno trascorso
e non perderti in lacrime sul domani che viene:
su passato e futuro non far fondamento
vivi dell'oggi e non perdere al vento la vita

Khayyam, poeta e filosofo persiano

Table of contents

PHASE 2

PHASE 3

INTRODUCTION AND RESEARCH OBJECTIVES

In the recent decades, many elements of the built environment are facing various types of damages and decays; hence exploring their conservation and preservation by compatible materials is demanding [1]. For a successful rehabilitation intervention, compatibility of the designated restorative materials with the substrate masonry is an essential requisite; sustainability and being economically friendly are recommended issues to be considered [2]. However, the low affinity of ordinary Portland cement (OPC) mortars/binders and modern polymer-based materials with historical substrates has been frequently discussed [3-6]. This incompatibility deals with lack of physical, chemical, and mechanical affinity of OPC mortars with old/historical masonry.

Availability and versatility of the repair materials are important items for restoration applications. However possession of these properties has made OPC mortars worldwide common construction materials; they can occupy considerable volumes in landfills and lead to environmental drawback. Moreover, energy consumptions and emissions regarding ordinary cement manufacturing are highly intensive due to the extreme heat required for their production. Producing one ton of OPC demands about 5 million kilojoules of energy, equivalent to nearly 180 kilogram of coal, and generates nearly a ton of carbon dioxide [7]. The most intense environmental problem is related to the increase of the mean air temperature [8], which is due to the increment of CO_2 in the atmosphere. The industry of construction is one of the largest and most active key players throughout European economy.

This manifests that many conventional mortars apart from lack of affinity with historical mortars are facing barriers for applications in new constructions. In order to respect the essence and feature of the originally applied materials in conservation, application of historic mixes as restorative renders is highly recommended as history and modern research has proved their performance and compatibility for restoration [9].

However, some traditional/ historical construction materials are non eco-friendly products, basically due to their high energy consuming components due to their production process or their compounds [10]. Hence introduction of more environmentally friendly restorative materials is necessary especially due to recent acceleration in global warming.

Although many modern historic mortars work well, the prices are quite high and each single additive of them targets a certain performance. Thus they are usually combined in utilization and increase the workload and final price**.** The economical considerations do place in an important part of conservation plans. Introduction of materials with economically friendly properties spread the possibilities to treat built environment as best practice within the conservation plan and maintenance routines. The astonishing costs of conservations do not only deal with historical sites and buildings and conservation materials developments do not neglect contemporary built environment. The rehabilitation of infrastructures and cultural heritage exhibits heavy costs. Since a huge part of architectural heritage elements and infrastructures are in need of constant conservation, their rehabilitation before occurrence of extensive damages is a hot issue to be dealt with [11]. Development of the low cost and sustainable repair mortars for rehabilitation of built environment including heritage and infrastructure is the concern of many scholars in fields of civil, materials, and cultural heritage. In order to broaden the conservation

domain the economical and environmental aspects should be improved with respect to conventional solutions; option of the additives sources from agro-food waste resources explores high sustainability as limits the dependency on natural resources [12,13].

In conservation of built environment, renders are among the most important applications as rather than aesthetical issue they protect the masonry in facing environmental treats such as humidity [14]. There are many deteriorated surfaces in need of restorative rendering with advanced compatible mortars (Figure 1). Such mortars rather than compatibility are recommended to have high indexes of performance, durability, availability, and sustainability.

Fig. 1. Example of degraded masonries in need of rendering with compatible mortars (Bobbio, Italy)

Another application that has a very frequent need in conservation of old deteriorated masonries is repointing (Figure 2). It was historically a common practice also, when the external part of the mortar joints was periodically renewed. Despite the apparent easiness of rendering and repointing, the new materials used for these applications should be carefully selected, as their compatibility with the existing masonry materials is essential to prevent negative consequences on the original mortars and bricks [15]. For instance, the use of hard and compact cement-based mortars frequently leads to mortar

detachment (especially when sulphates are released in the masonry due to rising damp), or causes corrosion and powdering of the surrounding bricks [16,17]. For this reason, it is usually recommended that repair materials match as much as possible with the existing ones, in terms of microstructural and physical properties (open porosity, pore size distribution, water absorption and water vapour permeability), mechanical properties (compressive and tensile strength, modulus of elasticity) and thermal properties (coefficient of thermal expansion) [18]. Even if it is usually recommended that restoration mortars be designed by simulating the historic ones [19], still using traditional raw materials and technologies does not assure the production of compatible restoration mortars [20], hence the utility of investigating novel alternative restoration materials comes out.

Fig.2. Examples of decayed masonries in need of repointing

Starting from the short introduction above, in this dissertation new historic waste-based mortars/pastes were formulated and manufactured and their microstructural and physical properties were determined, in order to investigate their compatibility with existing old/ historical masonries. In particular, properties such as open porosity and pore size distribution and, consequently, water absorption and water vapour permeability, are essential to guarantee that exchanges of liquid water and water vapour can take place between the masonry and the environment [15]. After application of the restorative material, if such exchanges were reduced, severe degradation might

take place. For these reasons, in the present study the mentioned properties were investigated for the new pastes/ mortars and their similarity with known as standard restorative mortars was evaluated, as this similarity is considered to be significant for the achievement of the compatibility requirement.

This dissertation includes three phases of valorization of potential restorative waste-based materials. The first phase deals with valorization of alkali-activated materials from brick waste for repointing of historic masonries; the results obtained from this phase of the dissertation are recently published as a research paper [21]. The two latter phases deal with valorization of organic additions in lime mortars for restorative rendering applications.

PHASE 1

VALORIZATION OF ALKALI-ACTIVATED BRICK WASTE FOR MASONRY REPOINTING

1.1 BACKGROUND AND RESEARCH AIM

Materials based on alkali activation are inorganic materials, mainly amorphous, obtained from activation of solid aluminosilicate sources by means of alkaline solutions [22-26]. When the solid precursors are mainly composed of silica and alumina (SiO_2+Al_2O_3 > 80%), activated materials are known as "geopolymers"; in the case where calcium-containing amorphous or crystalline phases are present in the precursors, materials produced by alkali activation are known as "alkali-activated materials (AAM)" or "inorganic polymers"[24]. This class of materials is receiving increasing attention in the field of civil engineering, because of the high potential exhibited by AAM: they have mechanical and microstructural properties similar (and in some cases even superior) to those of ordinary Portland cement but, at the same time, they have a much improved environmental impact [27-30].

The mechanism of AAM formation (or geopolymerization) is very complex and it is generally described as composed of three steps: (i) dissolution of solid aluminosilicate precursors in alkaline environment, as a consequence of breakage of covalent bonds Si-O-Si and Al-O-Si caused by OH^- groups, with the result that structural units with high reactivity are produced; (ii) accumulation and orientation of the dissolved units, that start to interact to

form a coagulated structure; (iii) condensation and hardening to an inorganic polymeric structure [28]. The nature and features of the final product of geopolymerization depend on the composition of the starting precursors. In the case of raw materials rich in SiO_2 and Al_2O_3 and poor in calcium (such as metakaolin), geopolymerization leads to the formation of a 3D-structure, composed of cross-linked SiO_4^- and AlO_4^- tetrahedra, where the negative charge is attributed to AlO_4^- by the positive charge of alkali ion (Na^+ or K^+) [31]. This structure is similar to that of zeolites, but without long-range order, i.e. the structure is amorphous. In the case of raw materials rich in calcium (such as blast furnace slag), Na^+ ions will be partially substituted with Ca^{2+} ions, so that a (N,C)-A-S-H gel is formed [28].

Among aluminosilicate sources that can be alkali-activated, metakaolin is often taken as a reference system, because of its very suitable oxide composition, very high reactivity, and because it contains no extraneous material [31,32]. Metakaolin is obtained by calcination of natural kaolin ($Al_2O_3 \cdot 2SiO_2 \cdot 2H_2O$), usually carried out at 700 °C. As metakaolin production involves much lower firing temperature than OPC (700 °C compared to 1450 °C) with 90% lower CO_2 emissions, production of metakaolin-based geopolymers stands out as more sustainable than OPC [26]. An even more sustainable alternative to metakaolin (and natural raw materials in general) is the use of industrial by-products and waste as precursors for AAM. In recent years, alkali-activation of fly ash, blast furnace slag, glass, ladle slag, ceramic waste, brick waste, incineration bottom ash, and hydrated-carbonated cement has been investigated [31-38]. Some of these by-products are currently already used in the cement industry as substitutes for OPC; however, while OPC substitutions in most of the cases range between 10-35%, AAM have the advantage of being produced entirely from waste materials.

Among other waste, the possible use of clay brick waste has recently been investigated [34,39]. Brick waste constitutes a huge percentage of construction and demolition waste in Europe (more than 50% in Spain [35]) and in other countries, hence their recycling is of strategic importance. Accordingly, the possible use of brick waste for production of several materials in the civil and building sectors has been investigated [40-43] including mortars, where brick dust was used mainly as a pozzolanic material for partial replacement of cement [44,45].

The possible alkali-activation of powdered clay brick waste has been investigated with curing at 65 °C and room temperature [39]. Mortars prepared using alkali-activated brick powder as binder and siliceous sand as aggregate, cured at 65 °C for 7 days, exhibited 30-50 MPa compressive strength, 12-20% open porosity (decreasing with increasing sodium silicate used for activation) and pore size increasing for increasing sodium silicate. The geopolymerization product was found to be an aluminosilicate gel, whose exact nature could not be clearly assessed. Sodium carbonate was found as well, as a consequence of excessive concentration of the activator. Crystalline quartz originally present in the starting brick waste powder was found to be largely unreactive, as expected. To promote the formation of a silico-aluminate network when the precursor is partially crystalline, the effect of using different amounts of sodium silicate for brick powder activation was investigated in a previous study [39]. Pastes obtained from activation at room temperature, and left to cure for 7 days, exhibited bulk density of 1.5-2.0 g/cm^3 and water absorption of 20-27%, respectively increasing and decreasing for increasing sodium silicate. This trend was attributed to the action of sodium silicate, that allows a higher degree of geopolymerization, in a similar way as found for room temperature activation of fly ash. Consistently with the higher degree of

geopolymerization, efflorescences composed of sodium carbonate were found to decrease for increasing sodium silicate [39].

In this phase, a preliminary study is presented about the feasibility of using pastes from brick waste alkali-activation for repointing existing masonries. In many historical and contemporary cases, while masonry was internally built with ordinary lime mortar, the joints external part was filled with a different kind of mortar, made with addition of some crushed brick. In this way, the pointing mortar acquired a more aesthetic appearance and a better durability than the inner part of the joints (due to the pozzolanic activity of brick dust): a typical example of this is illustrated in Figure 3. As discussed in the introduction, the compatibility of new repointing materials with old masonries is demanding to prevent the negative consequences on the original bricks and mortars [15]. Hence, it is usually recommended that repair materials match as much as possible with the existing ones, in terms of microstructural and physical properties. Even if in many cases restoration mortars are recommended to be designed by simulating the historic ones to assure the compatibility [19], still using traditional technologies does not guarantee a compatible restoration [20]; hence investigating novel alternative restoration materials is demanding.

The idea of using pastes from alkali-activation of brick waste for masonry repointing was firstly considered due to their aesthetical appearance, matching quite well that of traditional mortars containing brick dust, given their pink colour. In terms of composition, the new materials from brick waste activation may seem quite different from traditional materials; however several similarities between modern AAM and ancient binders may be found [28]. Indeed, in historic crushed brick/lime mortars, alkali-activation of silicates in brick fragments by $Ca(OH)_2$ has been suggested as the origin of amorphous C-S-H, formed at the crushed brick/binder interface and within discontinuities in

brick fragments, as the reaction product between activated silicates and $Ca(OH)_2$ itself [46]. Similarly, in mortars containing pozzolanic additions, the reaction between pozzolan and $Ca(OH)_2$ has been suggested as a consequence of the alkali-activation of the pozzolanic material by the alkaline solution created by $Ca(OH)_2$, that then reacts with the released silicate and aluminate monomers [47]. Moreover, the possible formation of proper aluminosilicate inorganic polymers as reaction products of pozzolanic material alkali-activation has been hypothesized as well [47]. The presence of zeolitic compounds in ancient binders has been suggested as the final product of a long term conversion of geopolymeric-like phases to zeolitic-like phases [28]. Consistent with the above-reported theories, $Ca(OH)_2$ is still sometimes used for alkali-activation of aluminosilicates, such as fly ash and metakaolin [48].

Fig. 3. Example of ancient repointing using a crushed-brick mortar [21]

To investigate the possible compatibility (in terms of chemical composition, as well as other features) between modern AAM and historical materials, a few studies has been carried out so far on the use of alkali activation for conservation of traditional materials, belonging to Cultural Heritage. Metakaolin-based geopolymers have been used as restoration materials for

reinforcement of a terracotta sculpture, exhibiting good results in terms of compatibility [49]. Basalt fibre-reinforced geopolymers (from activation of metakaolin and granulated blast furnace slag) have been investigated as possible materials for structural reinforcement of historic brick masonries, also in this case exhibiting good compatibility [50]. Moreover, alkaline solutions ($Ca(OH)_2$, NaOH, KOH) have been investigated as possible methods for consolidation of clay-rich soils used in earthen architecture (e.g. adobe), by formation of gel-like silicate cements with consolidating properties [51]. Recently, the feasibility of using mechano-chemical activation of quartz and kaolin for producing geopolymeric materials to be used as compatible restoration mortars for Cultural Heritage conservation has been investigated, with the aim of reducing risks that may be connected to the use of highly concentrated solutions on monuments [52].

Starting from the short review above, in this phase of the dissertation new alkali-activated pastes from brick waste were formulated and manufactured and their microstructural and physical properties were determined, in order to investigate their compatibility with existing masonries. In particular, open porosity and pore size distribution and, consequently, water absorption and water vapour permeability, are essential to guarantee that exchanges of liquid water and water vapour can take place between the masonry and the environment [15]. If such exchanges were significantly reduced after application of the repointing material, severe degradation might take place, for instance in case the evaporation of water coming from rising damp from the ground is significantly reduced or blocked [53]. Hence, in the present phase the mentioned properties were investigated for the new pastes and their similarity with traditional lime-based mortars was evaluated, as this similarity is considered to be significant for the soundness of the compatibility requirement.

Moreover, considering that efflorescences are usually found as by-products of the geopolymerization process and also considering that the soluble salts content in repointing materials should be as low as possible [15], the issue of efflorescence formation was specifically taken into account and its possible reduction by several strategies was investigated.

1.2 EXPERIMENTAL PART

1.2.1 Materials

Discarded commercial bricks, that could not meet the requirements for the market because of some physical/geometrical defect, were used as the source of brick powder. Discarded bricks were kindly supplied by Wienerberger S.p.A. (industrial plant of Villabruna di Feltre, Belluno, Italy). Bricks were ground by laboratory hammer and ball mill, so as to obtain a powder with desired fineness. The average particle size of the brick waste powder (BWP), determined by laser granulometry (Mastersizer 2000, Malvern Instruments), was about 10 μm.

The chemical composition of the BWP was determined by inductively coupled plasma optical emission spectrometry (Optima 3200 XL, Perkin Elmer). The crystalline phases were determined by X-ray diffractometry (Philips PW 1840 X-ray diffractometer) and the amorphous phases by Rietveld refinement (Bruker D8 Advance X-ray diffractometer). The chemical composition of the BWP is reported in Table 1. The amorphous content of the BWP is ~16%, hence much lower than that of an optimum geopolymer precursor such as metakaolin (~60%). The main amorphous phases in the

BWP are Al_2O_3 (4.71 wt%) and SiO_2 (3.04 wt%). The main crystalline phase is quartz, followed by calcite, albite and maghemite.

To modify the Al_2O_3 and SiO_2 amounts, sodium aluminate (Sigma Aldrich, technical grade, Na_2O = 40-45%, Al_2O_3 = 50-56%) and a 44% sodium silicate solution (Ingessil, Italy, SiO_2/Na_2O = 1.99) were used. In addition to the sodium silicate solution, a 8 M sodium hydroxide solution (prepared using NaOH pellets from Sigma Aldrich, assay ≥ 98%, and deionized water) was used as activating solution.

Table 1. Chemical composition and content of amorphous phases of the BWP [21].

	SiO_2	Al_2O_3	Na_2O	K_2O	CaO	MgO	Fe_2O_3
Overall amount (wt%)	58.00	10.64	0.60	1.85	12.36	3.88	4.82
Amorphous amount (wt%)	3.04	4.71	-	-	2.72	0.66	1.69

1.2.2 Samples mix design and preparations

As reported in Table 2, 5 different formulations were tested and each formulation was cured at 2 different temperatures, for a total of 10 sample types. For the 5 formulations cured at room temperature, the name of the respective samples starts with "R", while for the 5 formulations cured at relatively high temperature (50 °C), the name of the samples starts with "H". For each curing temperature, the different formulations are identified by two numbers (following "R" or "H"), indicating the SiO_2/Al_2O_3 molar ratio multiplied by 10.

For each formulation, the mix design is reported in Table 2, while the SiO_2/Al_2O_3, Na_2O/SiO_2 and Na_2O/Al_2O_3 ratios are reported in Table 3. Table 3 also reports the weight ratio between reactive and non-reactive fractions

(hence the ratio between the binding phase and the inert phase) and the weight ratio between liquid and solid fractions. In all calculations, the BWP amorphous fractions were considered as reactive (and hence computed in the oxides molar ratios), while the crystalline fractions were considered as inert. The SiO_2/Al_2O_3 ratio was taken as the primary parameter and varied from 1.4 to 0.4, by increasing amounts of sodium aluminate. Sodium aluminate was increased as the addition of aluminum oxide has been reported to reduce efflorescence formation [54].

Table 2. Mix design and curing temperature of the investigated samples [21].

Sample	Brick waste powder [wt%]	Sodium aluminate [wt%]	Sodium silicate solution [wt%]	Sodium hydroxide solution [wt%]	Added water [wt%]	Curing temperature [°C]
R14	64.5	2.3	5.1	6.6	21.3	22
R09	59.4	7.9	6.4	4.6	21.8	22
R08	57.9	9.3	6.7	4.5	21.7	22
R06	53.2	14.3	7.4	3.7	21.5	22
R04	50.8	18.5	4.3	2.6	23.8	22
H14	64.5	2.3	5.1	6.6	21.3	50
H09	59.4	7.9	6.4	4.6	21.8	50
H08	57.9	9.3	6.7	4.5	21.7	50
H06	53.2	14.3	7.4	3.7	21.5	50
H04	50.8	18.5	4.3	2.6	23.8	50

The sodium hydroxide solution was progressively decreased and the amount of sodium silicate solution was varied within a small range (Table 2), so as to maintain the Na_2O/Al_2O_3 ratio basically constant (0.7-0.8) and to have the Na_2O/SiO_2 ratio varying from 1.9 to 0.5 (Table 3). The amount of added water was varied a little (Table 2), so as to maintain basically constant the ratio between liquid fraction (comprising both the added water and the activating solutions) and solid fraction (Table 3). Accordingly, slight differences in the mixes workability were observed.

Samples were prepared by firstly mixing the alkali-activating solutions, 2 hours before sample preparation. Sodium aluminate was added to the cooled mixture of the activating solutions to avoid gelation in the mix. BWP was then gradually added to the solutions and, after mixing for 5 minutes in a planetary mixer, the slurries were casted in disc-shaped moulds (diameter 60 mm, height 20 mm) over a thick glass. Then, samples were manually vibrated for 20 seconds to remove entrapped air bubbles.

Table 3. Molar ratios between significant oxides, weight ratios between reactive and non-reactive fractions and weight ratios between liquid and solid fractions [21]

Sample	SiO_2/Al_2O_3	Na_2O/SiO_2	Na_2O/Al_2O_3	reactive/ non-reactive [w/w]	liquid/ solid [w/w]
R14	1.4	1.9	0.7	0.2	0.5
R09	0.9	1.2	0.8	0.3	0.5
R08	0.8	0.9	0.8	0.3	0.5
R06	0.6	0.8	0.7	0.4	0.5
R04	0.4	0.5	0.7	0.5	0.4
H14	1.4	1.9	0.7	0.2	0.5
H09	0.9	1.2	0.8	0.3	0.5
H08	0.8	0.9	0.8	0.3	0.5
H06	0.6	0.8	0.7	0.4	0.5
H04	0.4	0.5	0.7	0.5	0.4

Samples were finally cured in two different conditions, i.e. room temperature and 50 °C. Curing at relatively high temperature was performed because it has been pointed out as a possible strategy to reduce efflorescence formation [54]. Curing at 50 °C would be hardly feasible on a real masonry in the field, nonetheless it was investigated here to ascertain the role of temperature on efflorescence formation and microstructure development.

Samples cured at room temperature (R14-R04) were kept for the first 24 hours at 22 ± 2 °C and 40 ± 2% relative humidity, then demolded and cured for further 49 days in the same conditions. Samples cured at 50 °C (H14-H04)

were put inside impermeable plastic bags right after preparation; the plastic bags were then sealed to maintain relative humidity constant and put inside an oven at 50°C; after 24 hours, they were demolded and then again put inside impermeable plastic bags and subjected to the same conditions for further 13 days. The curing methods were designated with different lengths aiming at assessing both curing time and curing temperature effects. A schematic illustration of the binders synthesis is reported in Appendix A.

1.2.3 Samples characterization

Microstructure. For all formulations, mercury intrusion porosimetry (MIP) was used to determine the cumulative volume of mercury intruded into samples, the total open porosity (*OP*) and the average pore radius (r_{av}). The measurements were carried out on samples (~0.8 cm^3 volume) obtained from the disc-shapes specimens by chisel. A Carlo Erba 2000 Porosimeter, equipped with a macro-pore unit (Model 120, Fison Instruments, contact angle 141.3 °), was used.

Fig.4. Carlo Erba porosimeter

For selected formulations (R14, R04, H14 and H4), sample microstructure was observed in fracture cross sections, using a scanning electron microscope

(SEM) LEO "EVO 40XVP-M" Zeiss, equipped with an energy-dispersive X-ray spectroscopy (EDS) analysis system (INCA Energy 250, Oxford Analytical Instruments Ltd.). Samples were coated with gold to make them conductive. The above-mentioned formulations were selected to evaluate the effect of the SiO_2/Al_2O_3 boundary ratios (by comparing R14 with R04 and H14 with H04) and the effect of the different curing temperature (by comparing R14 with H14 and R04 with H04).

Efflorescence formation. At the end of the curing period, the formation of efflorescences over sample external surface was evaluated by visual inspection. The formation of efflorescences beneath sample surface (so-called "sub-efflorescences") was evaluated by observing sample fracture surfaces with a stereo-optical microscope (SOM) Olympus SZX10 at 40× magnification.

Water absorption. Water absorption by total immersion (*WA*) was measured on duplicate disc-shaped samples for each formulation. Samples were dried in oven at 100 °C for 24 hours before the test. After cooling and checking mass stabilization, the dry mass (m_{dry}) was recorded and samples were completely immersed in distilled water for 24 h. The mass corresponding to the "saturated surface dry condition" (m_{ssd}) was then recorded. Water absorption after immersion for 24 hours (WA_{24h}) was then determined as $WA_{24h} = [(m_{ssd} - m_{dry})/m_{dry}] \times 100$.

Fig.5. A sample under water absorption test

Water vapour permeability. Water vapor permeability was determined on triplicate samples for each formulation. The test was performed according to EN 1015-19 [55], in a conditioned environment at temperature of 22 ± 2 °C and relative humidity of 40 ± 2%. The disc-shaped specimens were placed and sealed on top of glass containers, filled with a KNO_3 saturated solution, so that a ~10 mm layer of air was left between the sample and the solution. The water vapor pressure difference between the air gap inside the container (where a constant pressure is maintained by the saturated saline solution) and the environment causes water vapor flow through the specimens. Mass loss as a function of time was recorded for 30 days and the water vapor diffusion resistance coefficient (μ) was then calculated according to the cited standard.

Fig.6. Permeability measurements

1.3 RESULTS AND DISCUSSION

1.3.1 Microstructure

The pore size distribution of samples cured at room temperature and 50 °C is illustrated in Figure 7. For both curing conditions, open porosity and bulk density were found to vary significantly as a function of the SiO_2/Al_2O_3 molar ratio (Figure 8).

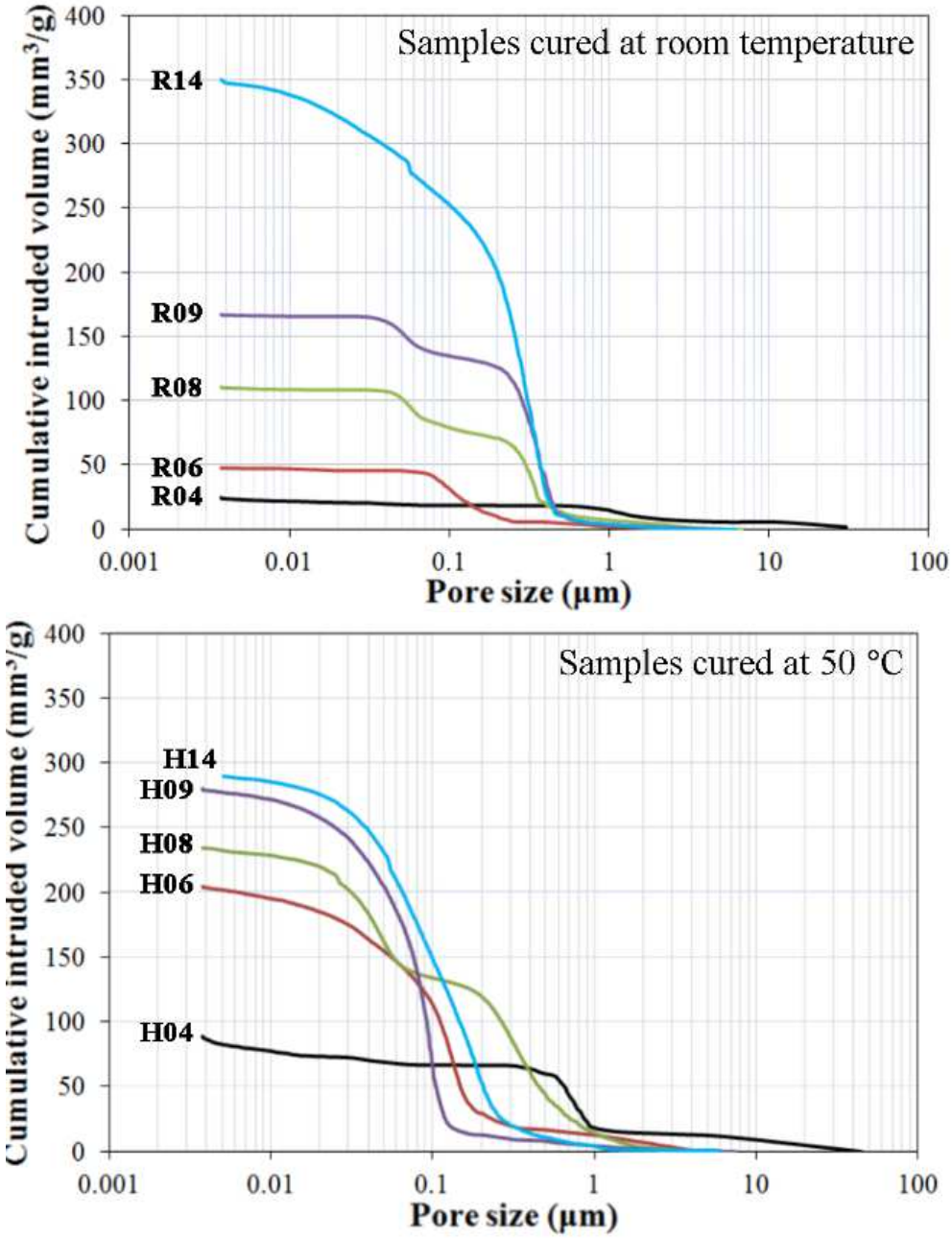

Figure 7. Pore size distribution of samples cured at 20 °C (up) and 50 °C (down) [21].

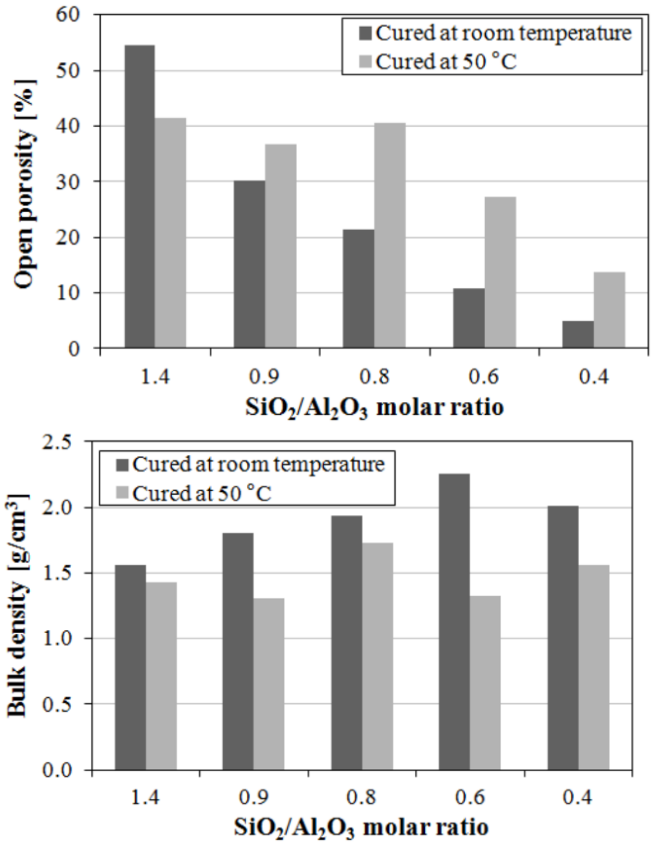

Figure 8. Open porosity (up) and bulk density (down) of samples as a function of SiO_2/Al_2O_3 ratio [21].

Samples cured at room temperature exhibited a progressive decrease in the volume of intruded mercury and in open porosity, as the SiO_2/Al_2O_3 ratio decreases. Passing from sample R14 to R04, a decrease in intruded mercury volume from 350 to 24 mm^3/g was registered. In terms of average pore size, a slight progressive decrease was found (from ~0.3 µm to ~0.1 µm), with the exception of sample R04, that exhibited a distinct behavior (average pore size ~1 µm). For sample R14, having SiO_2/Al_2O_3 = 1.4 (hence quite close to the ratio SiO_2/Al_2O_3 = 2 of metakaolin, usually considered as a reference system), the molar ration was suitable to reach a good level of geopolymerization. However, the low ratio between the reactive and the non-reactive fractions (amounting to 0.2, Table 3) led to a highly porous microstructure, because not

enough reactive fractions were available to form a continuous geopolymeric matrix embedding unreacted fractions. Consistently, SEM observation of sample R14 revealed numerous unreacted brick particles, as illustrated in Figure 9 (reporting back scattered electrons images). At higher magnification, smooth parts identified as geopolymeric gel and abundant unreacted brick powder were observed (Figure 10). To increase the ratio between reactive and non-reactive fractions, sodium aluminate was progressively added to the mixes, which resulted in progressive lowering of the SiO_2/Al_2O_3 ratio. So-obtained samples R09-R04 (classified as geopolymers in the high-alumina range, $SiO_2/Al_2O_3 < 2$ [49]) had reactive/non-reactive ratios ranging from 0.3 to 0.5 (Table 3) and actually exhibited a progressive microstructure densification (Figure 7). Accordingly, a denser microstructure was observed by SEM (Figure 10) and fewer unreacted particles were visible (Figure 9).

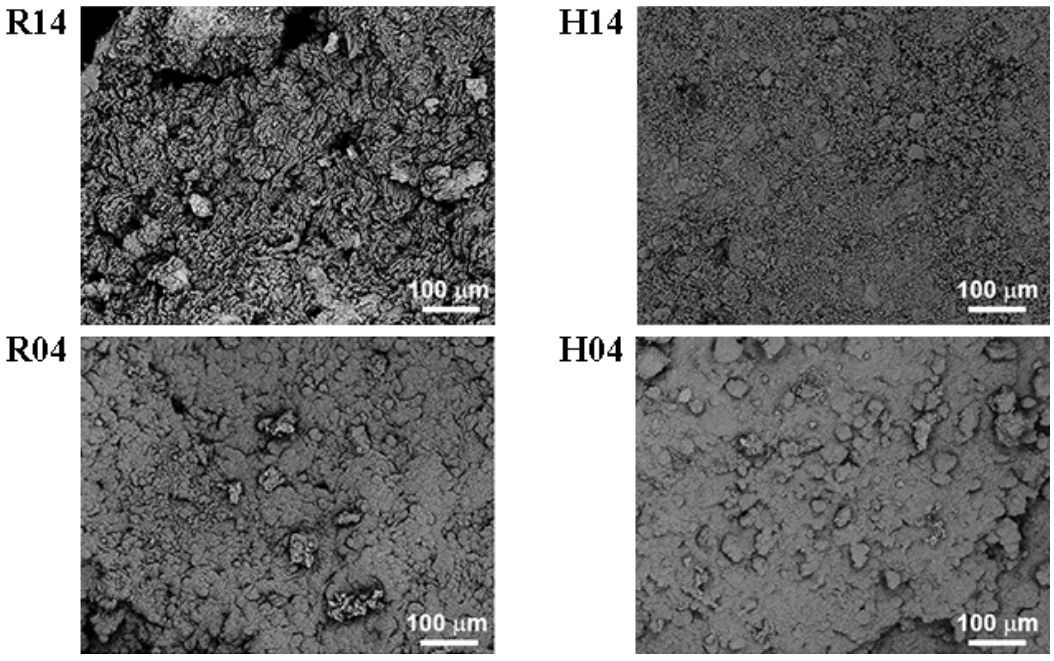

Figure 9. SEM micrographs of samples cured at room temperature (left) and 50 °C (right) (back scattered electrons, 300× magnification) [21].

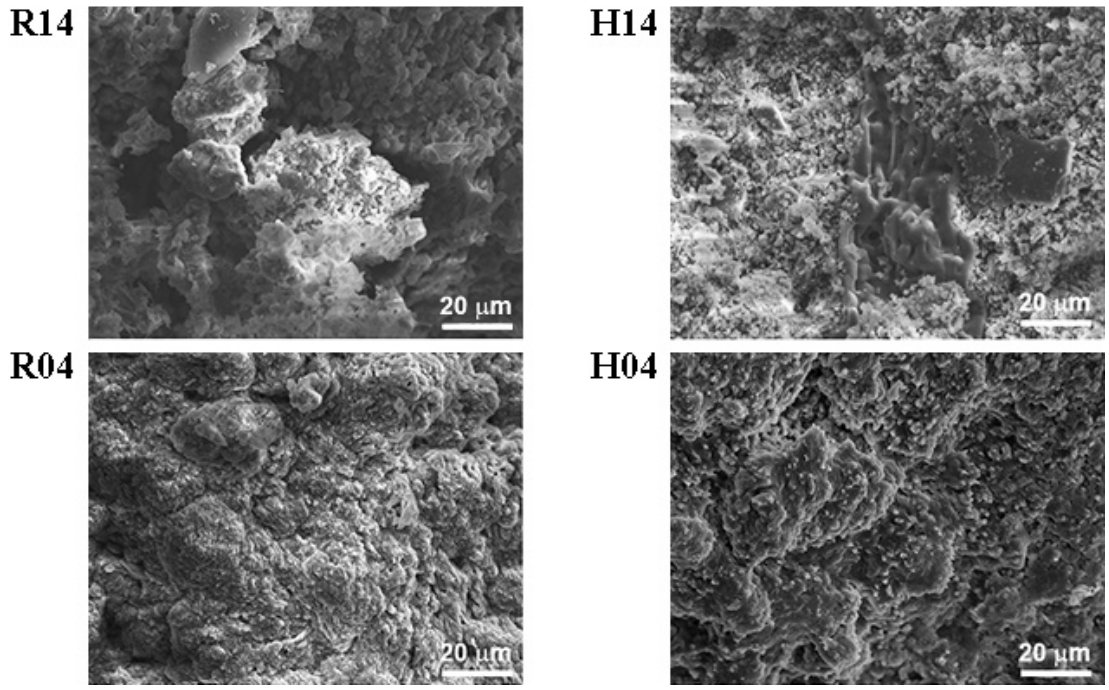

Figure 10. SEM micrographs of samples cured at room temperature (left) and 50 °C (right) (secondary electrons, 2000× magnification) [21].

Samples cured at 50 °C (with the exception of sample H04) exhibited a general increase in cumulative intruded volume and open porosity, with respect to samples cured at room temperature (Figures 7 and 8). This behavior is in agreement with the temperature effect reported in the literature for metakaolin-based geopolymers: when the curing temperature is increased, the hardening process proceeds more quickly and a larger volume of pores is formed, because no gradual filling of voids with geopolymerization products occurs (as would be the case for geopolymers cured at lower temperature) [26]. In terms of pore size, samples cured at high temperature mostly exhibited a reduction in the average pore radius. This is thought to be a consequence of the higher level of geopolymerization expected at higher temperature [54], also involving compounds that at room temperature remain unreacted and that give rise to efflorescence. As a result, after curing at high temperature pores are partly occluded and less effloresces are formed. SEM observation of samples

cured at high temperature confirmed that, for these samples, more gel formed from brick powder alkali activation, compared to samples cured at ambient temperature (Figure 10). Similarly to the case of samples cured at room temperature, also H14 exhibited more unreacted particles than sample H04 (Figure 9). In the case of H14, a decrease in cumulative intruded volume was registered, compared to R14. Considering that H14 also exhibited significantly less efflorescences than R14 (see 1.3.2), apparently curing at high temperature allowed some further reaction of fractions that at room temperature remain unreacted and form efflorescence on sample surface. As a result, H14 exhibited reduced porosity.

1.3.2 Efflorescence formation

At the end of the curing period, samples cured at room temperature exhibited some white efflorescences over sample surface (Figure 11). As assessed by SEM/EDS, these efflorescences are mainly composed of sodium carbonate, originated from carbonation of sodium oxide remained unreacted. The visible amount of surface efflorescences decreased for decreasing SiO_2/Al_2O_3 ratio (Figure 11). As expected from literature [54], adding an increasing amount of sodium aluminate (corresponding to a progressive decrease in the SiO_2/Al_2O_3 ratio) had the effect of reducing efflorescence formation, because a higher amount of Al_2O_3 is available for geopolymerization and a lower amount of sodium oxide remains unreacted. Anyway, SOM observation of sample cross sections revealed some white salt crystals in all the samples (Figure 12). The fact that, for sample R14, more efflorescences are visible on the surface and less in the cross section, while for sample R04 is the other way around, is thought to be a consequence of the different microstructure of these samples: in the case of R14, the high open

porosity and coarse pore size allowed efflorescences to be transported towards the surface during drying; in the case of sample R04, the dense microstructure favored salt crystals formation inside the sample.

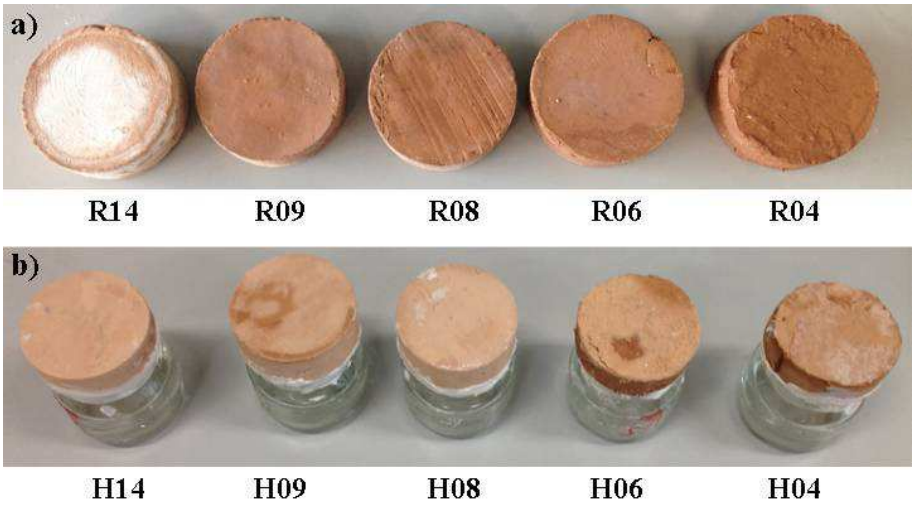

Figure 11. Efflorescences formed over the surface of samples cured at room temperature (a) and 50 °C (b) [21].

In the case of samples cured at 50°C, more limited efflorescence formation on sample surface was visible (Figure 11). This is in agreement with what reported in the literature, i.e. higher curing temperature allows a higher extent of geopolymerization, resulting in diminished efflorescences [54]. This was also confirmed by SEM observations (Figure 10). However, sparse white crystals were visible by SOM in cross sections of samples cured at 50 °C (Figure 12). Compared to samples cured at room temperature, the smaller average pore radius of samples cured at high temperature (Figure 7) presumably favored efflorescence crystallization inside the samples, rather than on the surface.

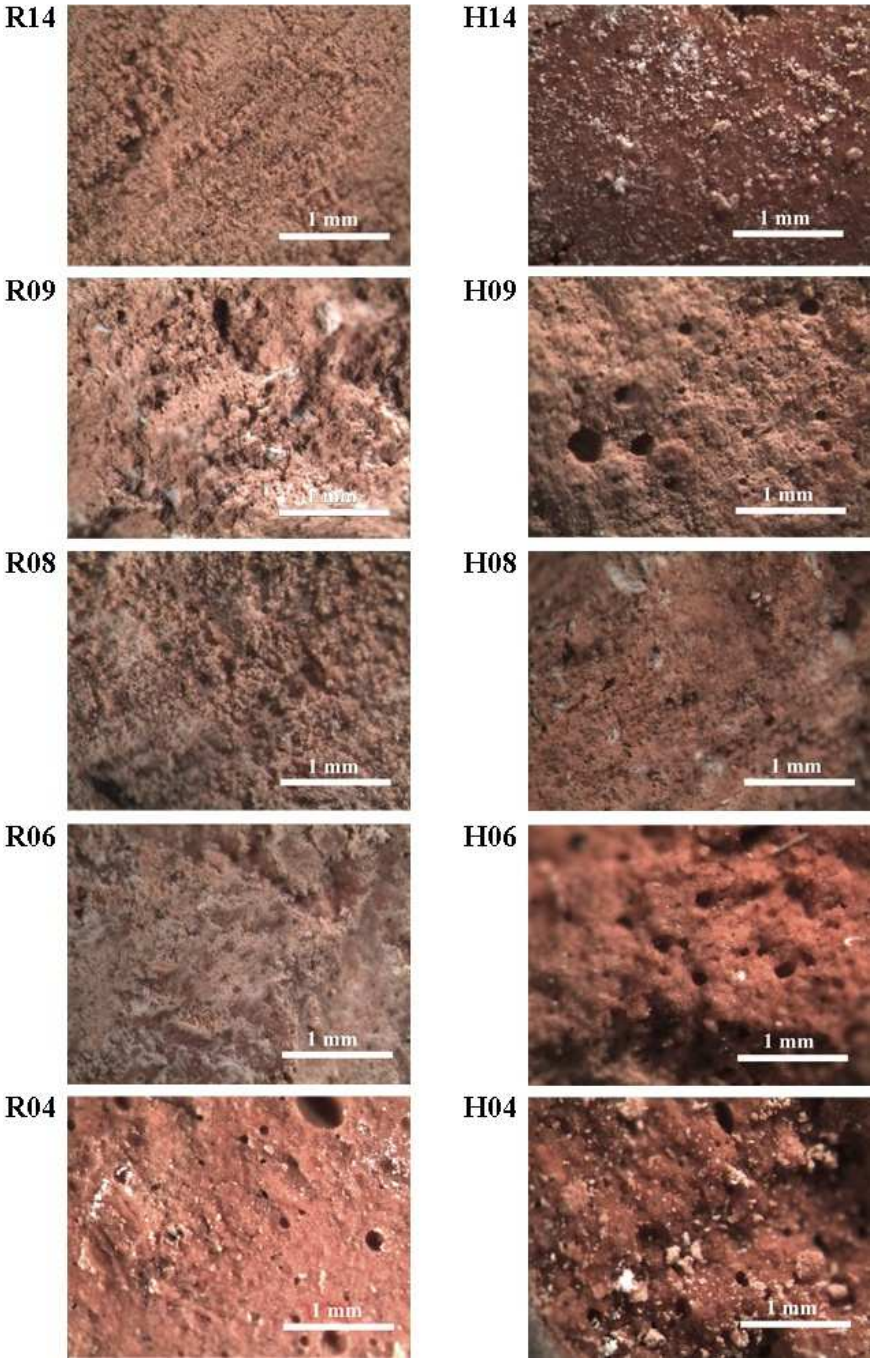

Fig. 12. SOM micrographs of fracture surfaces of samples cured at room temperature (left) and 50 °C (right) [21].

1.3.3 Water absorption

The results of the *WA* test are reported in Figure 13. All the samples exhibited high WA_{24h} values, ranging between 31-37% for samples cured at room temperature and 27-30% for samples cured at high temperature.

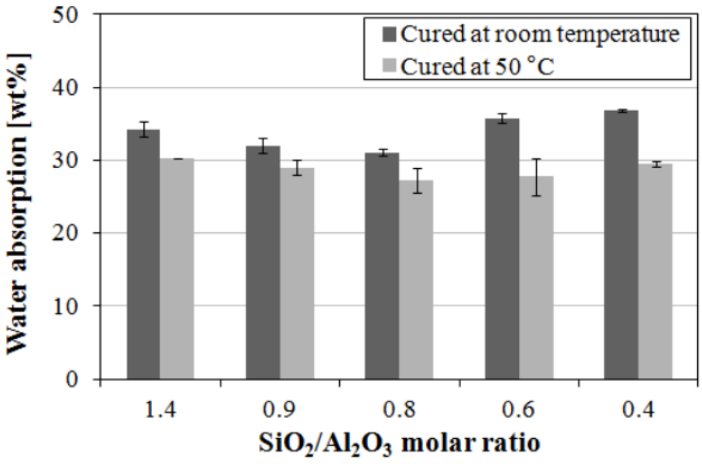

Fig. 13. Water absorption of samples as a function of SiO_2/Al_2O_3 ratio (values are averages for 2 samples, bars indicate standard deviation) [21].

The samples with SiO_2/Al_2O_3 ratios ranging from 1.4 to 0.8 exhibited a decreasing trend, in accordance with the trend found by MIP (Figure 7 and Figure 8). However, for samples with SiO_2/Al_2O_3 = 0.6 and 0.4, *WA* values were higher than expected. Different factors may have contributed to this. Firstly, in addition to pores detected by MIP, additional pores are present, with size exceeding the range of MIP detection (60 μm). For instance, pores with half millimeter-diameter are visible in the SOM micrograph of sample R04 (Figure 12), which may have significantly contributed to increasing *WA*. Secondly, *WA* test may have been partly affected by dissolution of sodium carbonate, highly soluble in water. As a matter of fact, probably some fractions were dissolved in water when samples were immersed for the *WA* test.

Dissolution of some soluble phases may be responsible for the high *WA* measured also for samples with low open porosity (such as samples R04 and H04) and may also explain why samples cured at high temperature exhibited a lower *WA* than samples cured at room temperature, in spite of having a higher open porosity. Indeed, samples cured at high temperature reached a higher level of geopolymerization (Figure 10), so that a lower amount of soluble efflorescences was formed.

1.3.4 Water vapor permeability

Water vapor permeability was evaluated in terms of water vapor diffusion resistance coefficient (μ), illustrated for the different samples in Figure 14. For all formulations and curing conditions, μ ranged between 4 and 10, with the exception of sample R04 (μ = 28). These relatively high μ values are in agreement with the high open porosity values found by MIP (Figure 7 and Figure 8). In the case of sample R04, the apparently extremely high μ value was however reproducible (triplicate samples gave very similar results). Such a high value is thought to be due, firstly, to the very dense microstructure of this sample (Figure 7) and, secondly, to the possible influence of sodium carbonate sub-efflorescences inside the sample (Figure 12). Being highly hygroscopic, sodium carbonate may have partly altered the test, which is based on weight loss measurement as a function of time (a scarce weight loss over time, corresponding to a scarce water vapor permeability, may have been registered because water vapor molecules were attracted and hold by sodium carbonate). The high impermeability of the surface of R04 hinders the CO_2 gain in the interior fragments of the material which is essential for alkali-activation process. Hence, lower levels of CO_2 gain in the inner fragments of the geopolymer-type material could led to decelerations in setting those fragments

and form layers with different levels of alkali-activation in this sample. Consequently, the existence of layers with various microstructures inside the material could considerably obstruct the vapor transition through the sample. Accordingly, the effect of curing at high temperature with the same nominal molar ratio (H04) exhibited high permeability of the material, due to modification of microstructure i.e. formation and increment of permeability pores.

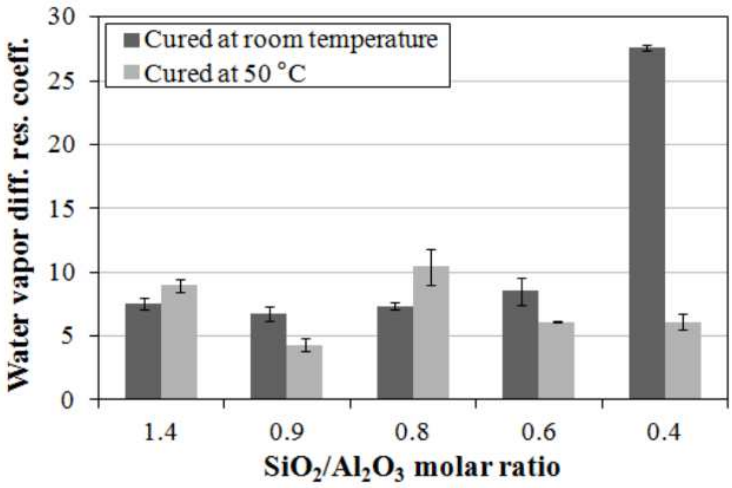

Fig. 14. Resistance to water vapor permeability of samples as a function of SiO_2/Al_2O_3 ratio (values are averages for 3 samples, bars indicate standard deviation) [21].

1.4 PRELIMINARY EVALUATION OF COMPATIBILITY AS REPOINTING MATERIALS

To evaluate the possible suitability of the alkali-activated pastes as repointing materials, their microstructural and physical properties were compared to those of historic lime-based mortars. A literature search on the range of variability of historic mortar properties was carried out and the

obtained results have been summarized in Table 4 [20,56,57]. In the case of water vapor diffusion resistance coefficient, no reference value for historic lime-based mortars was found in the literature, hence the reference value reported in the European Standard EN 998-1 [56] for "renovation mortars" was considered.

In terms of cumulative intruded volume and open porosity, a quite good match was found. With the exception of samples R04, R06 and H04 (that exhibited too low open porosity), all the other samples exhibited cumulative intruded volume and open porosity that fall within the range of lime-based mortars (which however exhibit remarkable differences among one another). Also in terms of pore size distribution, a good match was found between alkali-activated pastes and historic lime-based mortars. While samples cured at 50 °C exhibited pores with size slightly smaller than historic mortars, samples R14, R09 and R08 exhibited an average pore size very similar to that of lime/pozzolan, crushed brick/lime and hydraulic lime mortars. However, considering the high amount of unreacted brick powder discerned by SEM/EDS, found for sample R14, formulations with intermediate SiO_2/Al_2O_3 ratios (R09 and R08) seem preferable.

In terms of water absorption, all the prepared pastes were characterized by values (27-37 wt%) higher than those reported in the literature for "compatible" restoration mortars (19-22 wt%). However, as discussed in §1.3.3, the measured *WA* values were likely influenced by some dissolution of soluble efflorescences.

In terms of water vapor permeability, values of the μ coefficient are in all cases lower than the threshold for "renovation mortars" recommended by EN 998-1 ($\mu < 15$), except for sample R04 that exhibited a higher μ value. Anyway, sample R04 also exhibited too low open porosity, which led to identify this formation as not compatible with historic mortars.

All things considered, in terms of microstructural and physical properties, alkali-activated pastes with intermediate SiO_2/Al_2O_3 ratios (R09 and R08) appear as quite similar and hence potentially compatible with historic lime-based mortars. In the case of lime mortars with crushed brick (so-called "*cocciopesto*"), characterized by their pale pink color, the alkali-activated pastes investigated in this study also have a very good aesthetical compatibility. The term "aesthetical compatibility" here deals with appearance of these new binders that is similar to many historic materials such as cocciopesto.

However, a factor that actually limits the applicability of the alkali-activated pastes investigated in this study is efflorescence formation. Indeed, restoration materials causing efflorescence formation are unsuitable, not only because effloresces are unaesthetic, but mostly because they might migrate from the restoration material to the historic mortars and bricks, thus possibly causing additional damage [15]. Therefore, a further optimization of the mix design seems necessary, to reduce unreacted sodium oxide leading to sodium carbonate efflorescences.

Table 4. Reference values of microstructural properties of historic mortars [56] and physical properties of restoration mortars commonly considered as compatible [20,57] (n.a. = not available) [21].

	Lime	Lime/ pozzolan	Crushed brick/lime	Hydraulic lime
Cumulative volume [mm^3/g]	170-320	160-265	170-290	90-230
Open porosity [%]	30-45	30-42	32-43	18-40
Average pore radius [μm]	0.8-3.3	0.1-1.5	0.1-0.8	0.1-3.5
Water absorption [wt.%]	19-22	22	n.a.	19
Water vapor diffusion resistance coefficient [-]	<15	<15	<15	<15

1.4 CONCLUSIONS (PHASE 1)

In this phase of the dissertation, pastes from alkali-activation of brick waste powder were produced, characterized and evaluated as possible materials for repointing historic masonries. Five different formulations (having SiO_2/Al_2O_3 molar ratio ranging from 1.4 to 0.4) and two different curing temperatures (room temperature and 50 °C) were investigated. From the results of the study, the following conclusions can be derived:

- The open porosity was found to decrease for decreasing SiO_2/Al_2O_3 ratio. For SiO_2/Al_2O_3 = 1.4, the molar ratio was suitable for reaching a good geopolymerization level, but enough reactive fractions were available to form a continuous geopolymeric matrix embedding unreacted fractions. Progressive addition of sodium aluminate (causing the SiO_2/Al_2O_3 ratio to decrease down to 0.4) resulted in progressive microstructure densification.
- Efflorescence formation was found to decrease for decreasing SiO_2/Al_2O_3 ratio. Progressive addition of sodium aluminate reduced efflorescences because a higher amount of Al_2O_3 is available for geopolymerization and a lower amount of sodium oxide remains unreacted and forms sodium carbonate efflorescences upon carbonation.
- Curing at high temperature generally favored geopolymerization and reduced efflorescences formation, even if some sodium carbonate sub-efflorescences were detected (presumably because the reduction in pore size, consequent to curing at high temperature, favored efflorescences formation inside the samples, rather than on their surface).
- In general, high water absorption and high water vapor permeability were found for all the formulations (except for the sample R04, exhibiting low vapor permeability). However, both tests were likely influenced by the presence of sodium carbonate efflorescences, causing an increase in water

absorption (because of sodium carbonate solubility in water) and a decrease in water vapor permeability (because of sodium carbonate hygroscopy).

- As for the possible use of pastes from brick waste alkali-activation for repointing historic masonries, among the investigated formulations those with intermediate SiO_2/Al_2O_3 ratios exhibited potential compatibility with historic mortars. Indeed, in terms of intruded mercury volume, open porosity and water vapor permeability, samples R09 and R08 exhibited values falling in the range of historic lime-based mortars. However, further optimization of the mix design seems necessary to reduce the formation of efflorescences, which may be harmful for the historic mortars and bricks.

INTRODUCTION TO PHASES 2 AND 3

Lime has historically been an important material in construction since ancient times. The history of application of limes manifests their highest use before 18th century, when they were gradually replaced by hydraulic limes, and later in 20th century by ordinary Portland cement binders [4,5,58]. It is proven that application of the OPC cannot be an option for repair and rehabilitation of old buildings due to incompatibility problems frequently associated with the origin of the pathology in restoration of historical buildings. The low affinity of OPC binders/mortars with historical substrates has been frequently discussed [3,6,58-60]. On the other hand, chemical, physical and mechanical compatibility of lime mortars for restoration of historical masonries has been confirmed, due to their permeability and not very high compressive strength [61].

Lime mortars due to their slow carbonation, low internal cohesion and high porosity, have often been mixed with many different additives to modify their properties. Studies of ancient formulations demonstrate that various organic additives (such as cheese, sugar, egg, and organic fatty additives) have been used in the mortars in the past centuries [62]. These mixtures have been prepared in order to enhance one or some of their properties, such as setting time, adhesion, impermeability, hardness and porosity. Application of some fatty organic additives in the mixes which led to enhancements in the hydric properties of the lime mortars had been a historical solution [5]. Addition of different types of oils in lime mortars has been done by many scholars and the developments of hydrophobic properties were almost always observed [63-70].

As recent instances, Nunes [67-69] reported that hydraulic lime mortars added with metakaolin and enriched with linseed oil, manifested a remarkable capillarity reduction and consequently higher resistance to NaCl cycles. In some studies, the additives source was the food industry and possibly the agro-food wastes. This could bring superior sustainability to the agro-food system as a result of reduction of dependency on natural recourses [12,13,71] In most of the previous studies, the effects of unsaturation levels of the oils used as mortar additives are not studied. However, unsaturation extent of these additives can be a key factor in microstructural alterations and hydrophobicity of the final product.

Hydraulic properties of the air lime mortars could be achieved as a result of pozzolanic materials additions in lime mortars, as many ancient civilizations have contributed to development of limes with hydraulic properties, namely by being in contact with water [72]. “Cocciopesto” or crushed brick mortar is a material that goes back to the later Roman epoch and had applications as plaster on surfaces prone to humid conditions [73]. These mortars as outdoor rendering materials manifest an aesthetic appearance for historical masonries with promising durability and performance. The enhancement of lime mortars with hydraulic properties by adding pozzolanic materials, in terms of mechanical resistance and durability, especially in humid conditions with limited exposure to air, is indicated in the literature [6,74]. The studies by Donatello [75], Cachim [76] and Nunes [69] have demonstrated that a mixture of lime binders and pozzolans or amorphous siliceous materials enhances the characteristics of the mix.

As previously discussed in introduction, rendering applications are required for many old deteriorated exterior surfaces. To prevent damages to original masonries, the compatibility of the new materials designed for this issue with the substrate is essential [15]. In this phase of the dissertation, the feasibility

and compatibility of using hydrophobic waste-based lime mortars for rendering application in historic/old buildings are investigated and discussed. Mortars are characterized in terms of properties which are important for the application of restorative outdoor rendering, such as workability at the fresh states, calcium carbonate formation rates, pore size distribution, water absorption through capillarity, water vapor permeability, mechanical strengths and durability life cycles. The characterizations aimed at providing an insight into the contribution of the waste additives to the hydrophobicity, performance and durability of lime-based mortars, when compared to the conventional restorative rendering materials.

In the second phase of dissertation, application of various oils as additives in lime-based mortars with a focus on unsaturation level of the fatty acids has been studied. However, study of oiled lime mortars has been carried out by many scholars and enhancement of hydric properties of the mortars were almost always concluded. However, these researches generally report some disadvantages of oiled mortars such as permeability reductions and setting decelerations.

Other disadvantages of the conventional lime mortars have been listed as their low internal cohesion and their slow carbonation. To overcome these shortages the protein additives have been historical [62] and modern solutions [77] to accelerate curing and entrain air in mortars. Among historical mortar protein additives blood and albumen has been frequently listed [78]. The results of a recent study on traditional restorative blood lime mortars showed superior binding strength, increased hydric property, weather resistance, and carbonation speed than common lime mortars thanks to hydrolysis of blood proteins under alkaline condition [9]. However, in some older researches on traditional blood lime mortars, prominent developments due to additives were

not manifested [79]. Although several researches have been done regarding traditional blood mortars [80,81], contemporary studies on effects of albumen in traditional lime mortars -as a prevalent additive of ancient times- is not reported.

High price of application of modern synthetic additives in mortars can be magnified as each synthetic additive targets development a certain property and various synthetics are usually used at the same time [9]. In order to broaden the conservation domain the economical and environmental aspects should be improved with respect to conventional solutions; option of the additives sources from agro-food waste resources, explores high sustainability as limits the dependency on natural resources [12].

In the third phase of this dissertation, pulverized brick waste as a ceramic residue is the pozzolanic additive in lime mortars with hydraulic properties. Accordingly, other waste-based additives used in this study are spent sunflower cooking oil and albumen. The suitability of the mortars with parallel valorization of organic waste additives is discussed in the third phase, as assessment of their potentials as restorative rendering mortars.

PHASE 2
VALORIZATION OF SPENT COOKING OILS ADDITIONS IN HYDROPHOBIC WASTE-BASED LIME MORTARS FOR RESTORATIVE RENDERING APPLICATION

2.1 BACKGROUND AND RESEARCH AIM

In this phase of the dissertation, ground brick waste as a ceramic residue (the same material as §1.2.3) is used as a pozzolanic additive in lime mortars. According to the newest version of EN 459-1 [82] standard of building lime, some limes with hydraulic properties formerly classified with other names are now classified as formulated limes (FL) or hydraulic limes (HL) as a function of the pozzolanic content. According to this, the synthesized mortars prepared in the present study are defined in two groups: air lime mortars (AL) with or without spent cooking oils as additives, and lime mortars with hydraulic properties with or without spent cooking oils as additives. The latter group includes formulated lime mortars (FL) containing brick waste powder content=3.1 wt.% and hydraulic lime mortars (HL) containing brick waste powder content=6.2 wt.%. Two different percentages (1.5 and 13%) of two types of spent cooking oils (high-oleic acid oil and high-linoleic acid oil) were used as additives in synthesis of the three mentioned categories of lime mortars. The designated variety of oils in quantities and characteristics (different unsaturation levels) were aimed to study their effects on mostly physical and microstructural alterations of the mortars, respectively.

2.2 EXPERIMENTAL PART

2.2.1 Materials

The lime putty used for the present study is a commercial product (Candor®, supplied by Calceviva, Fasano, Brindisi, Italy), available in the Italian market and classified as CL 90S according to EN 459-1 [82]. The high calcium lime (CaO>98 % - 12 month aged and with 48.8 % of water content) and pure siliceous sand with normalized granulometry according to EN 196-1 [83] (particle size between 0.08 and 2 mm) where used to form the reference mortar specimens. The mineralogical composition of drained lime putty was performed by XRD Philips Diffractometer PW 1840, 40kV/20mA- Cu Kα radiation, and it detected portlandite as the major crystalline phase (Figure 15). The designated pozzolanic material was the brick waste powder described in §1.2.1.

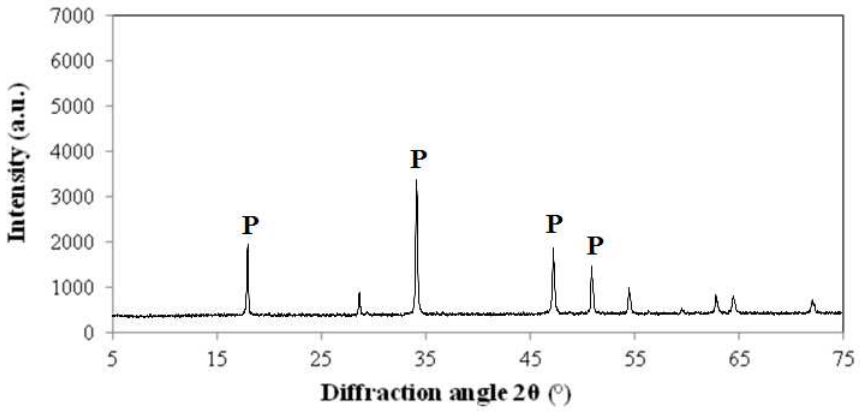

Fig.15. X-ray diffraction analysis of the lime putty; P: Portlandite

Table 5. Significant chemical characteristic of spent additive oils

Type of spent additive oils	Abbreviations	Oleic acid [%]	Linoleic acid [%]
High-oleic acid oil	O	85.42 ± 0.02	5.39 ± 0.01
High-linoleic acid oil	Q	68.43 ± 0.01	21.53 ± 0.01

Two types of sunflower oils (pure high-oleic one and a 70:30(v/v) mixture of high-oleic/high-linoleic ones) supplemented with natural additive antioxidants, were subjected to continuous frying of potato sticks at 180 °C (3 intermittent frying sessions/day) for 5 consecutive days, without replenishment. Frying was performed under these conditions in lab to mimic frying at catering level; at the end of the 5-day frying, both oils reached a percentage total polar compounds higher than the 25% limit set by the Circular of the Italian Ministry of Health (CM 1991, No.2568/91) [84] for fried oils to be discarded. The oils were added to the mixes at 1.5 wt.% according to literature [69] and 13wt.% to stress the effect of their unsaturation level. The fatty acid compositions of the spent cooking oils are shown in Table 5. The unsaturation level of high-linoleic acid oil is higher than high-oleic one. In chemical terms, high-oleic acids and high-linoleic ones are classified as monounsaturated (MUFAs) and polyunsaturated fats (PUFAs), respectively. MUFAs are fatty acids that contain only one double bond in their fatty acid chain and their other carbon atoms remain single-bonded. PUFAs are fatty acids that accommodate more than one double bond in their backbone (Figure 16).

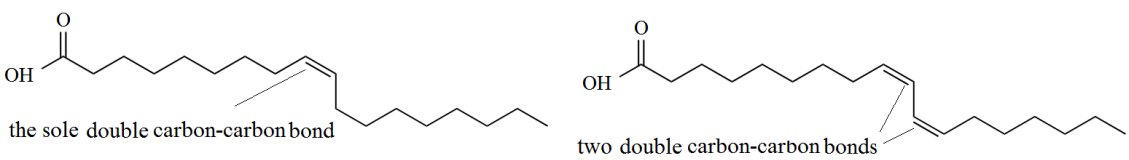

Fig. 16. Skeletal formulas of oleic acid (monounsaturated fat) (left); and linoleic acid (polyunsaturated fat) (right)

2.2.2 Samples mix design and preparations

The preparation of mortars consists in 3 main sets of air limes mortars (AL), formulated lime mortars (FL), and hydraulic limes mortars (HL) based on weight proportions of lime putty, sand, brick powder, and two types of additive spent cooking oils. The abbreviated sample names indicate the type of binder (AL, FL and HL), the type of the added spent cooking oil (O: high-oleic acid oil; Q: high-linoleic acid oil), and its amount (1.5 or 13 wt.%). For mortars with hydraulic properties, the addition of an amount of water was necessary to keep the water content of the samples equal to air lime mortar samples ones (12.5 wt.%) and consequently to achieve the same consistency of the reference mortar (AL). Table 6 and 7 exhibit the mass proportional compositions of non-oiled mixes and the mix designs of all the 15 prepared formulations, respectively.

Table 6. Mass proportional composition of the non-oiled mixtures

Sample	$Ca(OH)_2$	Brick waste powder	Sand	Added water	Added water/binder ratio
AL	1	-	3	-	0
FL	0.75	0.125	3	0.125	0.14
HL	0.5	0.25	3	0.25	0.33

A Hobart mortar mixer at low speed was used to prepare mortar samples. Lime putty and aggregates were mixed for 3 minutes and after 20 seconds pause, the mixture was blended for additional 3 minutes to prepare reference mortar (AL). Regarding the preparation of mortars with hydraulic properties (FL and HL sets), lime putty, brick waste, aggregates and water were mixed in the automatic mixer for 6 minutes to prepare FL and HL. The total water contents deals also with water content of the used lime putty.

Table 7. Mix design of the investigated samples

Sample	$Ca(OH)_2$ [wt.%]	Brick waste powder [wt.%]	Sand [wt.%]	Added water [wt.%]	Additive spent oils [wt.%]	Type of spent oil
AL	25.0	-	75.0	-	-	-
ALO1.5	24.6	-	73.9	-	1.5	O
ALQ1.5	24.6	-	73.9	-	1.5	Q
ALO13	21.7	-	65.3	-	13.0	O
ALQ13	21.7	-	65.3	-	13.0	Q
FL	18.8	3.1	75.0	3.1	-	-
FLO1.5	18.5	3.0	73.9	3.0	1.5	O
FLQ1.5	18.5	3.0	73.9	3.0	1.5	Q
FLO13	16.3	2.7	65.3	2.7	13.0	O
FLQ13	16.3	2.7	65.3	2.7	13.0	Q
HL	12.5	6.2	75.0	6.2	-	-
HLO1.5	12.3	6.1	73.9	6.1	1.5	O
HLQ1.5	12.3	6.1	73.9	6.1	1.5	Q
HLO13	10.9	5.4	65.3	5.4	13.0	O
HLQ13	10.9	5.4	65.3	5.4	13.0	Q

Spent cooking oil additions occurred for all the mortar types as follows: the oil and a minor portion of lime putty were manually blended for 3 minutes in a plastic beaker to effectively increase the homogenization of the mix; then this amount was added to the rest of the mix in the Hobart mixer and mixed for 6 min. The dispersion of oils in the mixtures was visually assessed and a sound homogeneity was observed. Oils additions in mortars generally respect their aesthetic integrity without considerable changes in their gloss and color [62]. Industrial refining of cooking oils makes them more stable and suitable for high-temperature cooking and also removes their flavor and color (resulting in a very pale color); hence, in every category, color changes were not observed by naked eye.

Fig. 17. Mortars preparation and casting

The mortars were molded in prismatic steel casts (40 ×40 ×160 mm) for capillarity and mechanical tests, in disc-shaped plastic molds (diameter = 60 mm, thickness = 20 mm) over a thick glass surface for permeability and durability assessments, and in cylindrical plastic molds (diameter=30mm, height=50mm) for calcium carbonate determination and mercury intrusion porosimeter (MIP) measurements. The freshly molded mortar samples were placed inside a basin (T=22 ± 2 °C, RH=98± 2 %) for 6 days, to accelerate their initial setting. After this period, the samples were demolded. The formulated and hydraulic lime samples containing brick waste as pozzolanic addition were cured in the same conditions for their whole curing period (2 years). The air lime samples were cured in the lab (T=22 ± 2 °C and RH=50±5 %) for 2 years in order to promote their natural carbonation process. A schematic illustration of the mortars synthesis is reported in Appendix B.

Fig. 18. Samples preparation for permeability measurements

2.2.3 Samples characterization

Workability. The workability of the mortars was assessed according to EN 1015-2 [80] in two synthesis rounds before their casting (flow table test). The reported values are average of two measurements from the formula:

$$100\ \frac{d_m - d}{d}$$

where d_m is the average of the two diameters measured with calipers and d is the lower diameter of the truncated cone.

Fig. 19. Mortars consistency characterization

Calcium carbonate determination. The calcium carbonate determination was assessed by a Dietrich Fruhling calcimeter after 60, 120 and 180 days of curing. The test specimens were taken from both surface and internal part (depth of ca. 20 mm) of cylindrical samples (diameter=30 mm, height=50 mm). Considering the designated application of rendering, test specimens taken from the surface were also tested after 2 years of curing. The calculation of $CaCO_3$ content of the samples is based on the released CO_2 from chemical reaction between the sample and hydrochloric acid. The reported values are averages of 2 measurements.

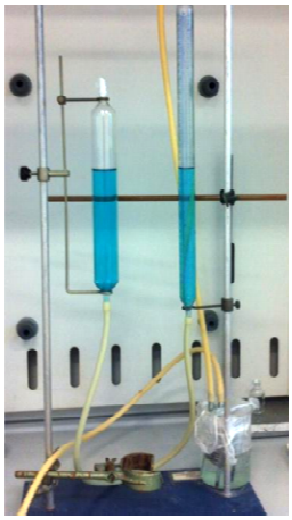

Fig. 20. Dietrich Fruhling calcimeter (gasometer)

Pore size distribution. Porosity measurements by mercury intrusion porosimeter (MIP) were carried out after 120 and 180 days of curing, in order to determine the values of total pore volume and pore size distribution of the lime mortars as was explained in §1.2.3.

Hydric properties. The hydric behavior of lime mortars towards water and water vapor were investigated in terms of capillarity and water vapor permeability measurements after 120 days of curing. Capillarity measurements were performed according to EN 1015-18 [86] on prismatic samples (40 × 40 × ~80 mm). The capillary coefficients of the samples were calculated as the mass of water absorbed between 10 and 90 min, per area unit and square root of time. Water vapor permeability of the mortars was examined on 3 samples for each mix design as was explained in §1.2.3.

Fig. 21. Capillarity measurements

Mechanical properties. Measurements of compressive strength were performed by an Amsler-Wolpert 100 KN device by constant displacement rate of 50 mm/min, according to UNI 196-1 [83]. The results are averages of two measurements on cubic samples (40 × 40 × 40 mm) after 180 days of curing. Dynamic elastic modulus test (Young's modulus) was performed on prismatic samples (40 × 40 × 160 mm) after 180 days of curing. The values of dynamic elastic modulus (E_d) were calculated as averages of 3 measurements according to the formula $E_d = V^2.\rho$, where V is the pulse velocity, measured by a Matest instrument with 55 kHz transducers and ρ is the material density.

Fig. 22. Compressive strength characterization

Fig. 23. Dynamic Elastic Modulus test

Optical microscopy. Optical microscopy was carried out on the fracture surfaces of the mortars after 180 days of curing to investigate their microstructure. The images were collected at 25x magnifications, using a continuous zoom stereomicroscope Olympus SZX10 with a digital camera.

Surface wettability. To assess the surface wettability of the mortars, the contact angle test was carried out according to EN 15802 [87] by a theta optical tensiometer after 180 days of curing. Contact angle θ is a quantitative measure of wetting of a solid, which is geometrically defined as the angle formed by a liquid. The reported values are averages of 3 measurements.

Freeze-thaw resistance. In order to test the surface durability of the mortars as outdoor rendering materials, 3 disc-shaped specimens (diameter=60 mm, thickness=20 mm) for each formulation, were subjected to 10 freezing-thawing cycles after 180 days of curing. The specimens were immersed in water for 1 hour, kept at a temperature of 22 ± 2 °C and a relative humidity of ≈ 40 ± 2% for 15 hours and then frozen at −20 ±2 °C for 8 hours (Table 8). The selected cycle was aimed to simulate a daily cycle in a cold environment. Superficial alterations were qualitatively investigated as an assessment of their suitability for outdoor rendering.

Table 8. A single freezing-thawing cycle (24 h)

Step	Temperature	Water immersion	Time for each step
Step 1	22 ± 2 °C	Yes	1 h
Step 2	22 ± 2 °C	No	15 h
Step 3	-20 ± 2 °C	No	8 h

2.3 RESULTS AND DISCUSSION

2.3.1 Workability

Workability values of the mortars are reported in Figure 24. FL and HL mortars exhibited a significant increase in workability with respect to the air lime mortars AL. Such increase can be due to the presence of brick waste powder as well as the added water. High workability values are very important for mortars for restoration purposes as they ease their applications.

For AL and HL mortars the addition of spent cooking oils always caused a decrease in the workability, which is more evident for AL series. Such a behavior is in agreement with effects of additive oils reported in literature [64,67]. The spent cooking oils cover the aggregates and the solid particles of the binder, leading to an increase in the cohesion among the particles and the formation of a less workable product. This physical phenomenon balances the increased workability due to extra/kneading water contents and it was not affected by the different types of oils, but generally from their amounts. However, in case of FL mortars apparently the optimum kneading water/binder ratio was obtained; hence almost all of the added water was consumed by the brick dust. Therefore, in case of FL mortars oils additions did not adversely decrease their workability values.

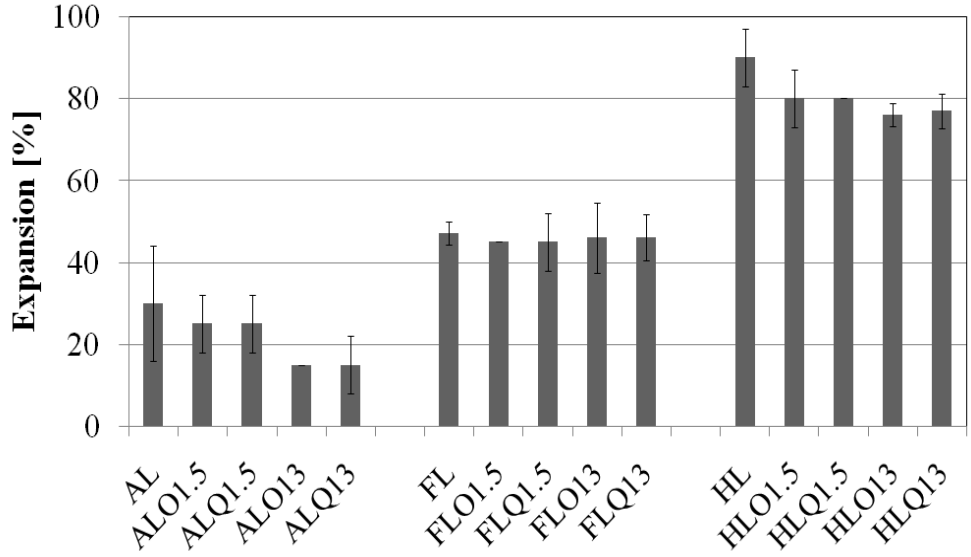

Fig. 24. Workability of the investigated mortars

2.3.2 Carbonation rate

Calcium carbonate formations on both surfaces and internal parts (taken from depth of ca. 20 mm) of the mortars were studied after 60, 120 and 180 days of curing as reported in Figures 25 and 26, respectively. The reported data demonstrate the calcium carbonate due to carbonation of calcium hydroxide present in the mortars. For FL and HL the calcium carbonate content due to the brick powder (ca. 4.2 % as determined by calcimetry measurement) was previously subtracted.

The more exterior surfaces of lime mortars demonstrate higher carbonation than their interior parts, as a consequence of being prone to humidity and CO_2 from the environment. As the aimed application of this study is rendering, the interest was calcium carbonate formation rate of superficial levels or finishing surface of the mortar; hence the formation of $CaCO_3$ in surface fragments of

the mortars has been additionally monitored after 2 years of curing. However, the comparison of the carbonation of internal parts and surfaces can be interesting in terms of assessment of the carbonation rates and permeability analogies.

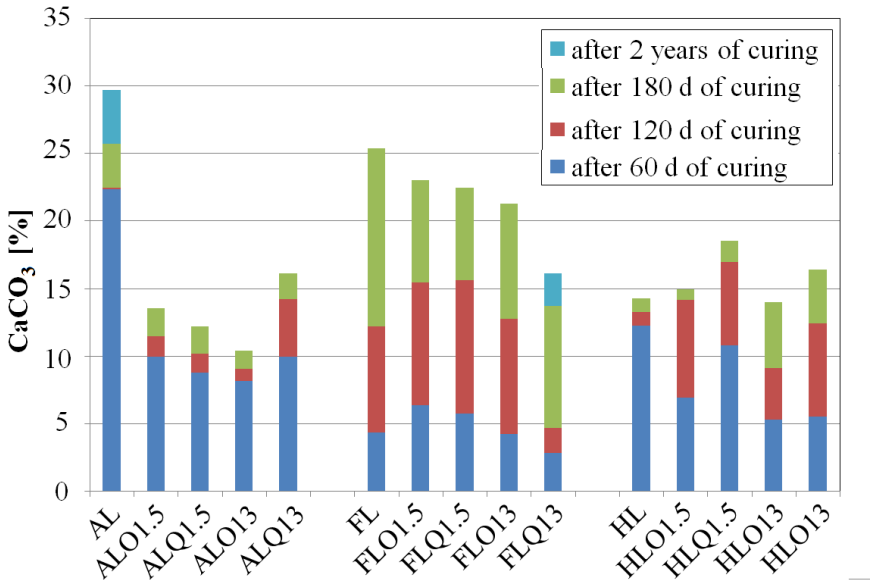

Fig. 25. Calcium carbonate formation of limes at the surfaces of mortars

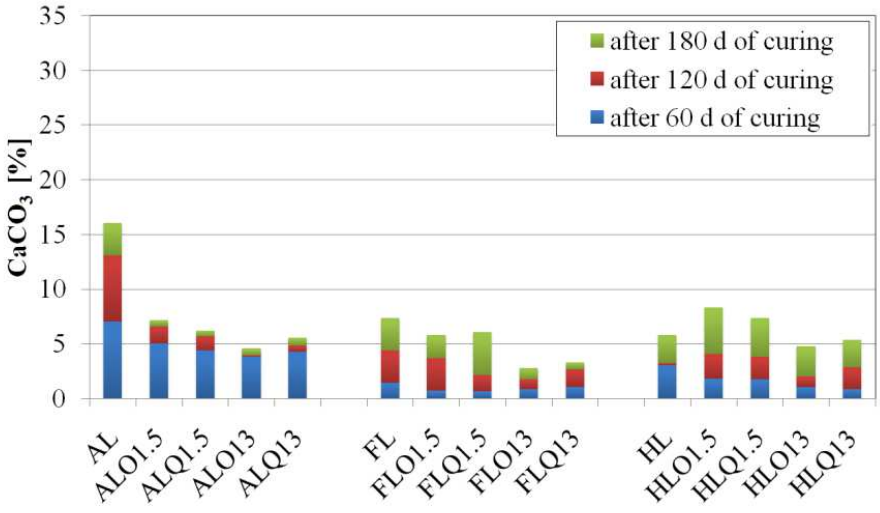

Fig. 26. Calcium carbonate formation of limes at the internal fragments of the mortars (depth of ca. 20mm)

The surfaces of AL mortars exhibited their major carbonation in the first 60 days of curing; they implemented 80-90% of their carbonation in this period. The non-oiled AL sample remained the only studied air lime mortar that exhibited extra carbonation after 180 days of curing. In case of FL and HL, calcium carbonate formation generally accelerated after 60 days due to slower setting through hydration reactions. The non-oiled FL mortar demonstrated a low level of carbonation after 60 days; however, after 180 days of curing it exhibited the highest level of calcium carbonate. For almost all of the FL mortars, the carbonation ceased before the age of 180 days as they did not exhibit extra $CaCO_3$ formation up to age of 2 years. The FL mortars displayed only 13-22% of their $CaCO_3$ formation in their first 60 days of curing and 30-45% of this process in the following 120 days. The only mortar with different $CaCO_3$ formation behavior in this group was the FLQ13, which exhibited low carbonation in the first 120 days of curing and consequently this process was not ceased by the age of 180 days.

The surface fragments of HL mortars exhibited a slightly higher rate of calcium carbonate formation than the FL mortars. The hydration process for formation of $CaCO_3$ in lime products with hydraulic properties is essentially slower than the carbonation process in air lime mortars. This explains the lower initial $CaCO_3$ formation rates determined for FL and HL than that one determined in AL mortars.

The additive spent cooking oils significantly decelerated the carbonation rate in AL mortars. Non-oiled FL mortar exhibited high calcium carbonate formation after 180 days of curing; nevertheless, the FL mortar containing the highest amounts of high-linoleic acid oil (FLQ13) presented the lowest calcium carbonate content among the formulated lime mortars. Initial calcium carbonate rate in oiled HL mortars showed a decrease with respect to non-oiled

HL sample; however, they generally reached the same amount of calcium carbonate of non-oiled HL mortar after 180 days of curing.

In general, the addition of spent cooking oils decreased carbonation, but its effect was more evident in AL mortars than in FL and HL samples where the occurrence of pozzolanic reactions already hindered CO_2 penetration. Nevertheless, 1.5 wt.% oil additions were found to exhibit slighter decreases in carbonation/hydration rates compared with higher extent additions.

Calcium carbonate formation at the internal fragments of mortars (Figure 26) demonstrated significantly low values due to limited CO_2 gain. As for the superficial carbonation, AL mortars exhibit higher carbonation than FL and HL mortar according to its higher content of calcium hydroxide. For FL and HL, pozzolanic reaction occurs between $Ca(OH)_2$ and brick powder thus creating a more effective barrier to CO_2 penetration and less calcium hydroxide available for carbonation.

2.3.3 Open porosity and pore size distribution

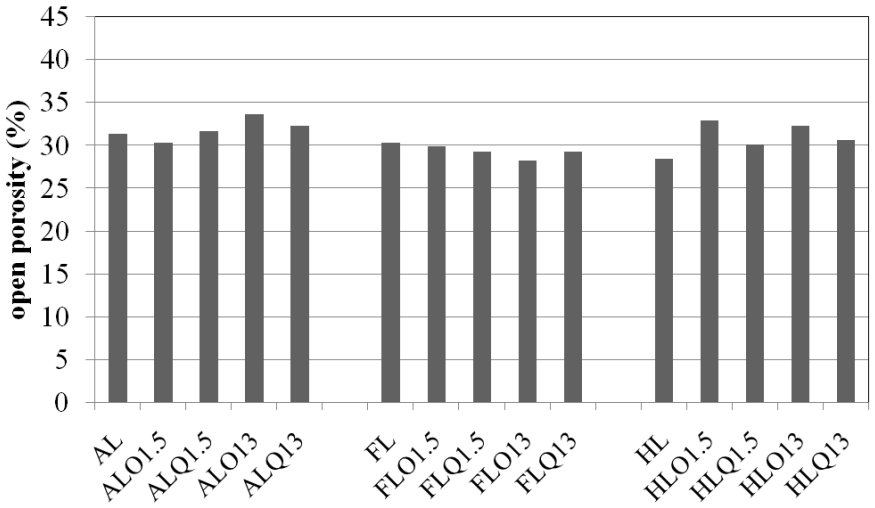

Fig. 27. Total open porosity of the investigated mortars determined by MIP at 180 days

The total open porosity (TOP) of the investigated samples determined by MIP at 180 days of curing is reported in Figure 27: the three different mortar types without spent oil addition exhibit similar values in the range 28-32 %. For AL mortars TOP slightly increases when the spent oil content is 13 wt%, but it remains almost unchanged when spent oil is not included or present in small amount (1.5%). On the contrary, for FL mortars spent oil does not enhance TOP even when the content is 13 wt%. For HL samples, the addition of spent oil leads to the highest increase in TOP and such increase is particularly evident for the mixes containing high-oleic acid oil.

As reported elsewhere addition of oils to mortars leads to formation of air macro pores [69] that many of them are probable to be out of the MIP detection range (60 microns). As previously discussed, rheology of FL mortars induced the probability of the optimum kneading water/binder ratio due to consumption of all added water by the brick dust. Therefore, formation of air voids in oiled FL mortars was not evident. Compared to air lime mortars, the effect of oils on microstructure of hydraulic mortars is more evident as the concentrations of fatty acids are higher since the water is consumed. However, lower reactivity of high-oleic acid oils than high-linoleic ones could lead to production of less and smaller air voids and keep them inside MIP detection range and consequently register a higher TOP value.

The graph of pore size distribution determined by MIP at 180 days of curing for AL, FL and HL samples are reported in Figures 28, 29 and 30, respectively. In accordance with literature, the AL mortars (Figure 28) exhibit low porosities with radius lower than 0.05 μm, which are mostly manifested in limes with hydraulic properties and phases such as calcium silicate hydrates [83]. Addition of high amounts of oil (ALO13 and ALQ13 samples) promoted

the highest cumulative intruded volume as well as the high content of pores with dimension in the range of 0.05-0.3 μm. These samples exhibited decreases in the pores with radius greater than 0.5 μm when compared to non-oiled AL.

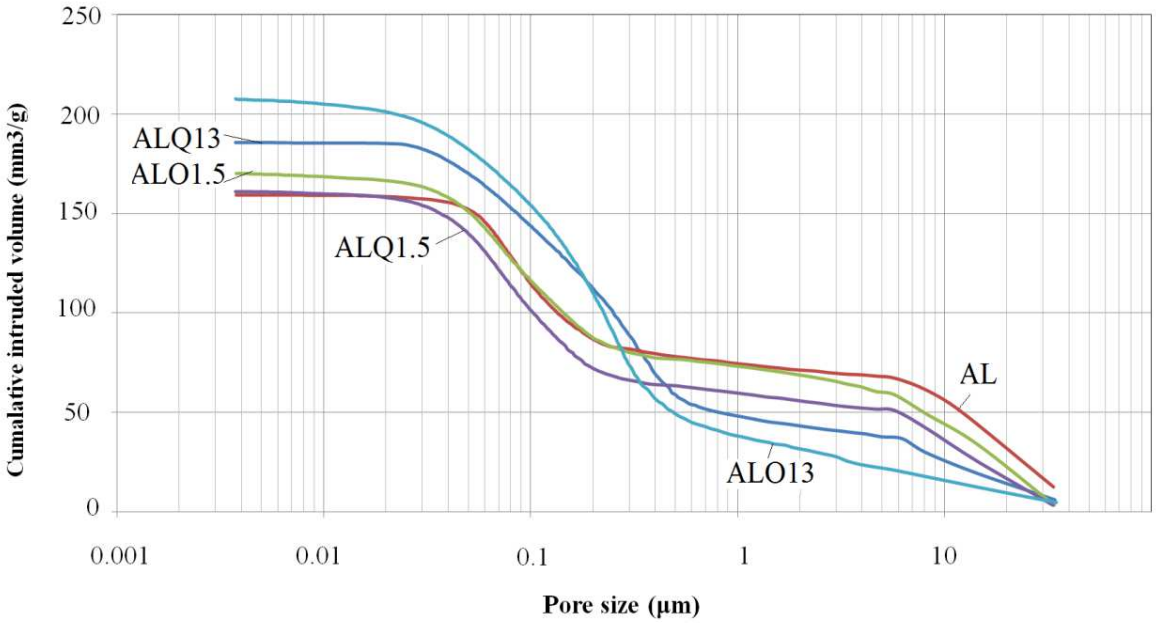

Fig. 28. Pore size distribution of air lime mortars at 180 days of curing

The pore size distribution of FL mortars (Figure 29) shows that all samples, regardless the oil content, have a quite similar trend and total cumulative intruded volume, which is generally lower than the one determined for AL mortars according to pozzolanic reactions occurring between brick waste and calcium hydroxide.

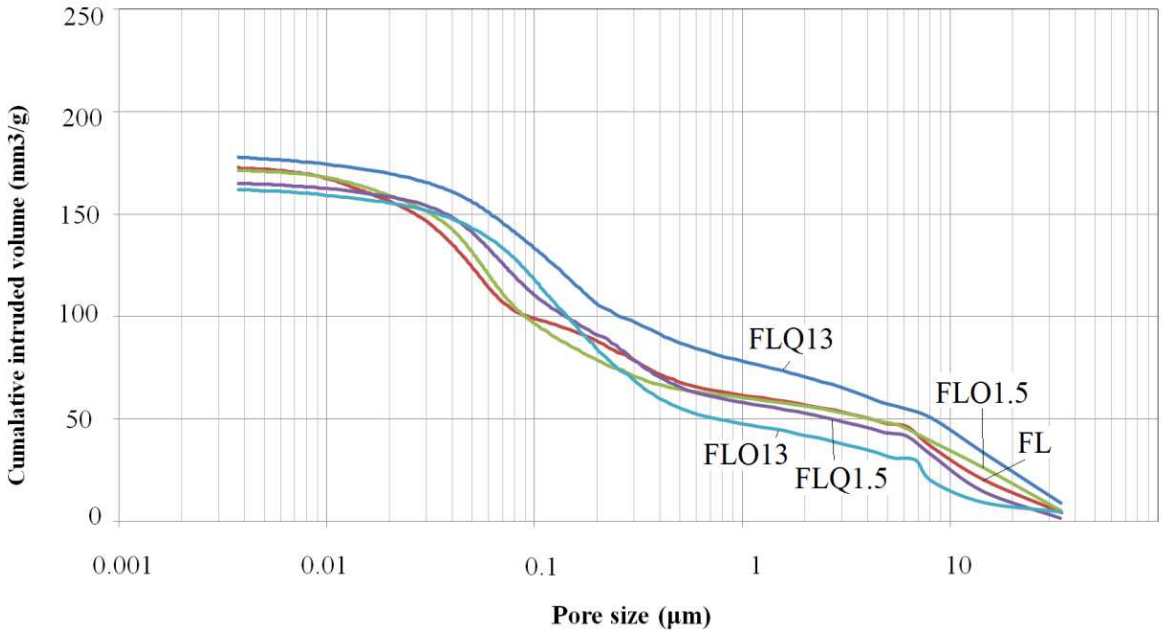

Fig. 29. Pore size distribution of formulated lime mortars at 180 days of curing

HL mortars exhibit pore size distribution and total cumulative intruded volumes more similar to AL than to FL samples (Figure 30). Although hydraulic reactions should occur and refine pores structure as it happens for FL samples, the high porosity here determined can be ascribed to the high content of water added in HL mixes.

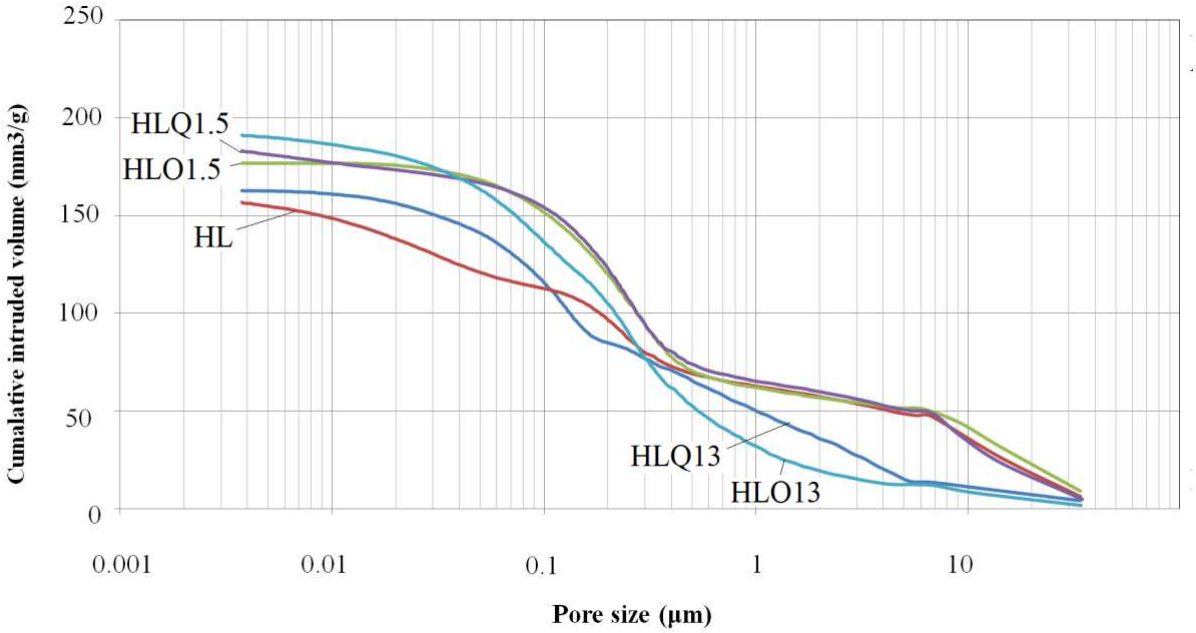

Fig. 30. Pore size distribution of hydraulic lime mortars at 180 days of curing

Generally, additions of higher percentage (13%) of oils demonstrated reductions in pores greater than 0.5 µm, after 180 days of curing. This effect was more evident in mortars with more saturated oil (high-oleic acid oil) additions, also confirmed in MIP assessment after 120 days. Nevertheless, these microstructural modifications were exhibited in case of 13 wt.% high-linoleic acid oil addition only after 180 days of curing. In other words, high-oleic acid oils caused the microstructural modifications to occur faster than case of addition of the same amount of high-linoleic acid oils. This effect of saturation level of the additive oils is also evident in results of previous researchers. A study of Ventolà [5] accounted that lime mortars with 5% olive oil (contains high MUFAs/ high-oleic acids) caused a reduction of roughly 48% in pore volume with respect to its reference after only 28 days of curing. Moreover, in a study of Křivánková [89] on linseed oils additions (contained high PUFAs/ high-linoleic acids) to lime mortars, no significant reduction in

pore size was reported at the age of 90 days; however after 180 days many pores of the oiled mortar were shifted towards smaller pore size.

2.3.4 Hydric properties

The behavior of lime mortars towards water and water vapor were investigated in terms of water absorption through capillary phenomenon and water vapor diffusion resistance coefficient as shown in Figures 31 and 32, respectively.

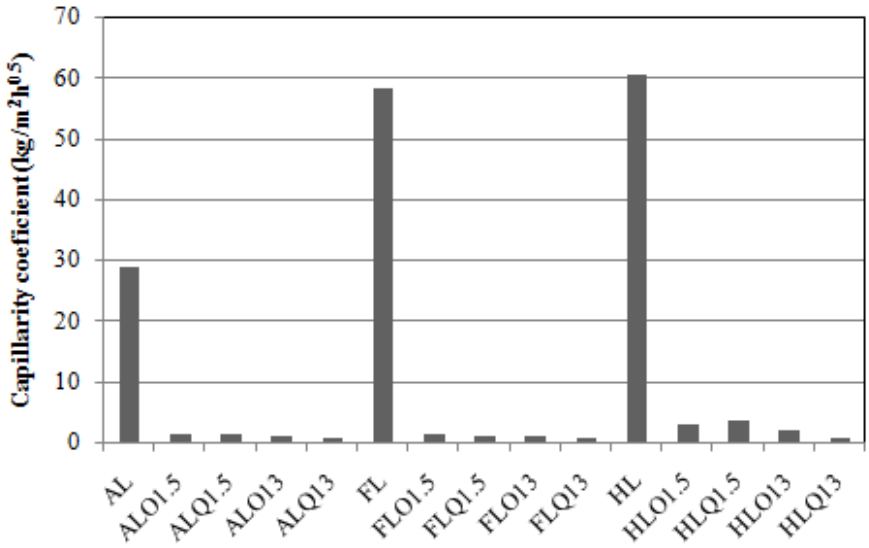

Fig. 31. Capillary coefficients of the investigated samples at 120 days of curing

High capillarity coefficients are registered for the non-oiled mortars as water can easily move in the vertical suction pores [90]. Their high capillarity can be additionally ascribed to their potential capillary pores that are greater than the mentioned MIP detection range. Comparing these data with the literature, the capillary coefficients of the lime mortars formulated with brick-waste results significantly higher than values for lime-metakaolin mortars

[67,69]. This can be due to less reactivity of brick powder with respect to metakaolin [21]. However, the contribution of pore size distribution in water intakes through capillarity can be substantially related to hydrophilic cavities.

The addition of spent cooking oils in the lime mortars exhibited a significant hydrophobic effect through capillarity, despite the formation of capillary pores in oiled mortars. Thirty-sixty times capillarity reduction was observed with the addition of spent cooking oils in mortars. This is due to the fact that the capillary suction cannot take place through vertical tunnels of pores with hydrophobic internal surfaces. As elsewhere reported [64], the internal surfaces of pores coated with layers of fatty materials turned their hydrophilic cavities into hydrophobic ones. The probable restriction of the interconnectivity of the capillary pores in the oiled mortars can be another important reason for such reductions.

For AL mortars, the decrease of capillarity coefficients was slightly more than the one determined when linseed oil was added to air lime mortars by Čechová [64] and Nunes[67,69]. For FL and HL oil containing samples the results were significantly more pronounced than those reported in previous studies where the same amount of linseed oil was added to lime-metakaolin mortars [69]. Such differences could be partly attributed to the higher unsaturation level of fatty acids in linseed oil with respect to the spent oils here used. The advanced hydrophobicity of mortars enriched by oils containing high unsaturated fatty acids is reported in literature [63,64,67]. The chemical reactivity of the high-linoleic acid oils is due to their triglyceride molecules by the double bonds of the unsaturated acids [91,92]. This unsaturation allows them to react with the oxygen of air and with one another to form a polymeric-shaped network [91]. The triglycerides present in the unsaturated oil break down to glycerol upon being mixed with the alkaline lime binder. Due to high

coordination of carboxyl group of the fatty acids with the present calcium, the fatty acids will be confined inside the lime mortar and water repellency will be created by the hydrophobic part of the molecules [63,67].

Therefore, polyunsaturated fats bring superior water repellency to lime mortars with respect to monounsaturated fats, due to their higher number of double bonds and superior reactivity with oxygen of the air (Figure 16).1.5 wt.% oils additions led to an adequate degree of hydrophobicity.

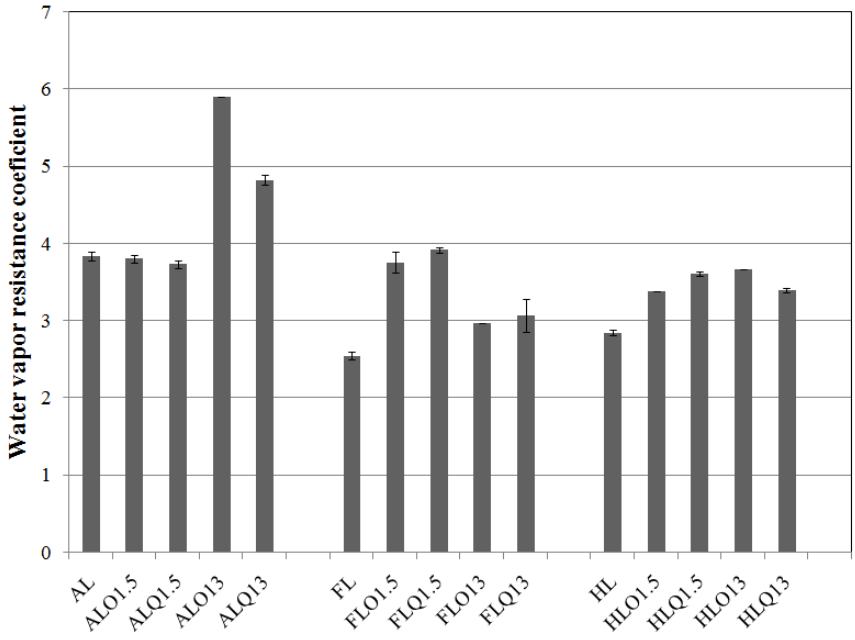

Fig. 22. Resistance to water vapor permeability of the investigated samples at 120 days of curing

Water vapor impermeability or the water vapor diffusion resistance coefficient for all the formulations ranged between 2.6 and 5.9.

In case of non-oiled lime mortars, specific ranges of pores corresponding to pores greater than 10 μm and between 0.421 and 1.778 μm can highly contribute to water vapor permeability of the mortars [93]. Pore size

distribution analysis in Figures 28-30 showed the determined content of permeability pores of non-oiled AL, FL and HL as 46.16, 74.79 and 66.93 mm^3/g, respectively. Accordingly, the non-oiled FL sample demonstrated the highest permeability among non-oiled mortars, due to its extent of permeability pores. The low impermeability values are in agreement with the high open porosity values obtained from MIP measurements (Figure 27).

A general increase of the water vapor diffusion resistance coefficient for the mortars containing added spent oils was observed. This effect was higher in AL (ALO13 and ALQ13) and FL (FLO1.5 and FLQ1.5) mortars. This is mainly because of the microstructural alterations in presence of oils. The reduction of permeability pores [93] for ALO13, ALQ13, FLO1.5, and FLQ1.5 mortars registered in Figures 8-9 explains the mentioned increased impermeability values. However, physically speaking, oils are also probable to affect the interconnectivity of the pores and consequently hinder their water vapor permeability. For HL samples, the oil presence improved impermeability regardless of the type and amount of oil. The reduced permeability here is proposed to be due to the restriction of the interconnectivities of the permeability pores.

It was concluded from calcium carbonate formation rates studies (Figure 25) that the addition of spent oils hindered the carbonation of mortars. The decreases in permeability of oiled mortars can be a convincing reason for decelerating their carbonation rates due to obstruction of the carbon dioxide. This could explain why AL and FL mortars exhibited decreases in their carbonation values; conceivably, this effect was higher in AL mortars. Accordingly, ALO13 sample showing the highest impermeability value demonstrated the lowest carbonation rate among air lime mortars. The mortars with higher impermeability exhibited lower carbonation/hydration rates at

depth of ca. 20 mm (Figure 26) with respect to non-oiled samples, due to lower interaction of their internal parts with air and water vapor.

Generally, the increased open porosity of the mortars with addition of spent cooking oils did not lead to permeability improvements, due to the hydrophobic carboxylates that covered their pores. Accordingly, 1.5 wt.% oils additions caused a lower impermeability increment with respect to the higher extent ones. The literature confirms the increase of impermeability of lime mortars by organic fatty additives, such as olive oil [5].

The favorable water vapor diffusion resistance coefficient patently depends on the desired applications of the mortars. Permeable rendering materials can facilitate the draining of the humidity inside the masonry, and therefore this is a very promising value for restoration applications [94]. However, the decreased permeability of the investigated mortars is still a proper value as a perquisite of restoration materials according to the European Standard EN 998-1 as "renovation mortars" [57]. According to this, water vapor diffusion resistance coefficient for "renovation mortars" can have a value lower than 15 [57].

2.3.5 Mechanical properties

Compressive strength and dynamic elastic modulus values of the investigated mortars are reported in Figure 33. The values of the compressive test for AL, FL and HL mortars without spent oil additions are very similar; for AL sample the reported values are in accordance with some previous studies [95,96]. The introduction of water in the mix of FL and HL leads to reach low mechanical performances which were only partially compensated by the pozzolanic action of the brick waste powder. A slight increase in mechanical

properties of the lime mortars was observed when formulated with brick powder. Some studies reported that formulated lime mortars with metakaolin addition [97,98] could reach a compressive strength up to 20% higher than that of lime mortar without hydraulic properties. This difference could be again ascribed to the namely low reactivity of brick powder due to its higher crystalline content than metakaolin; therefore less reactive silicates contributed in hydraulic products formation through pozzolanic action.

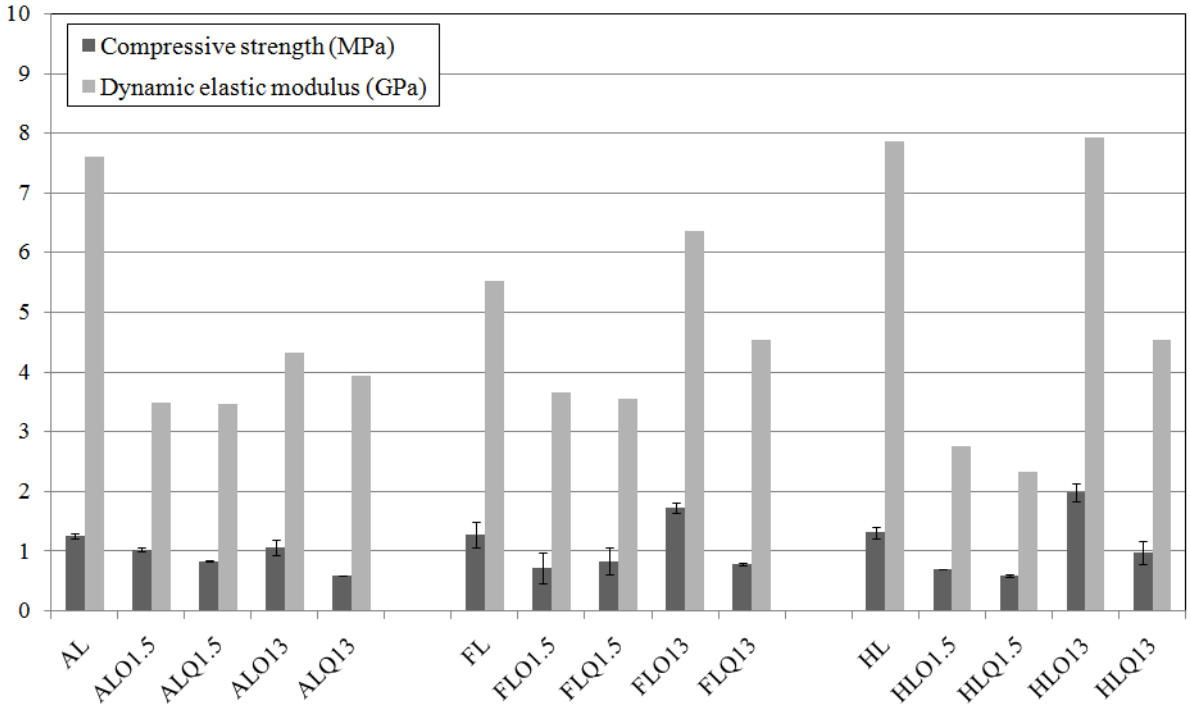

Fig. 33. Compressive strength and dynamic elastic modulus of the investigated samples at 180 days of curing

The compressive strength values of air lime mortars exhibited reductions with addition of oils. The study of Nunes [67] concluded the same result from application of linseed oil in air limes. However, in the present study the addition of high-oleic acid oils in large amount (13%) in FL and HL mortars

shows an increase in the compressive strength values of relevant samples FLO13 and HLO13.

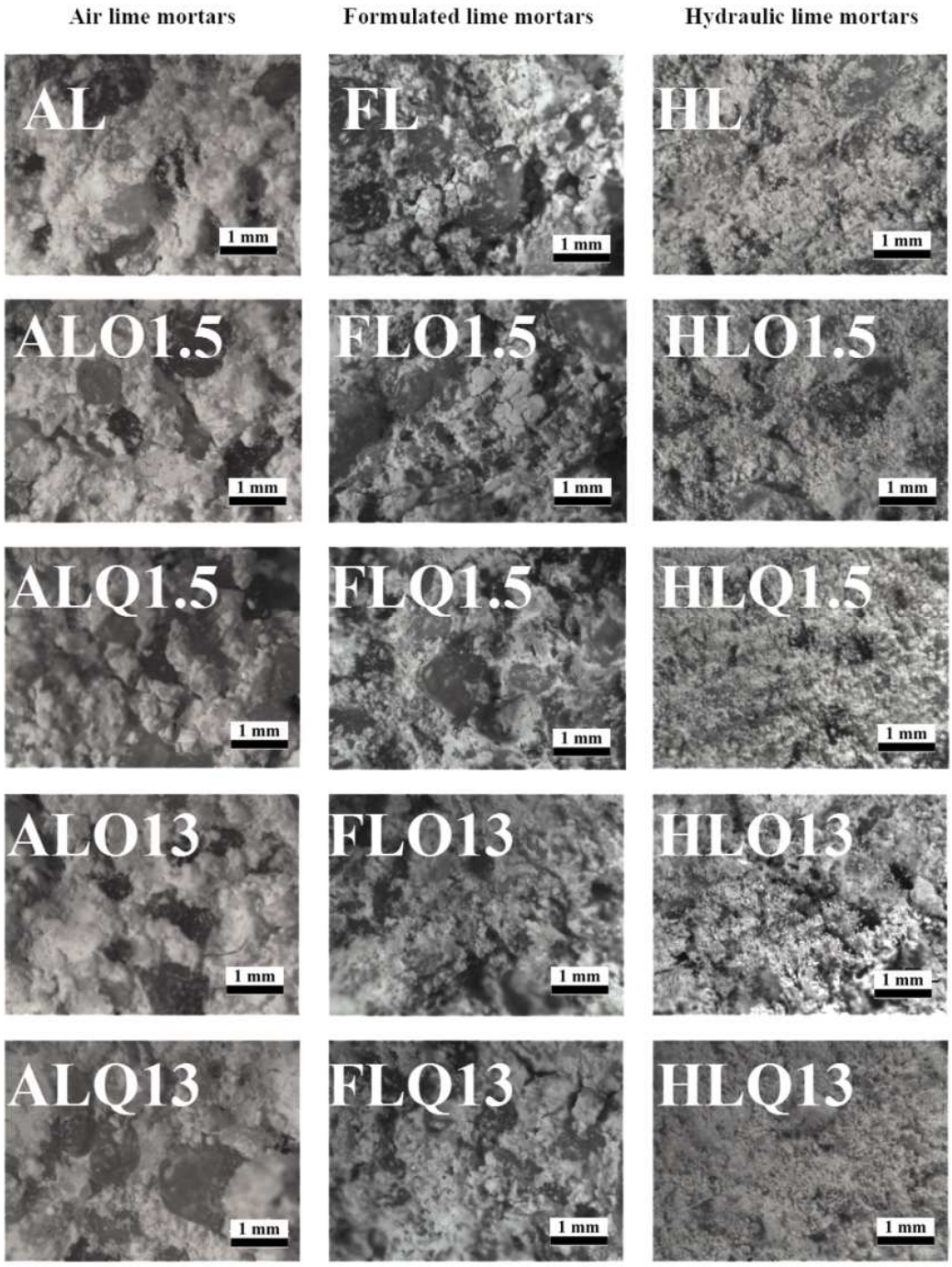

Fig. 34. SOM micrographs of the fracture surfaces of the samples at 180 days of curing

The SOM micrographs (Figure 34) indicated the preventive role of oil addition to mortars against formation of shrinkage cracks; a similar enhancement has been previously seen and interpreted in the study of other organic fatty additives used in lime mortars with hydraulic properties [64]. Figure 34 demonstrates formations of large (~0.3 mm diameter) spherical pores in the hydraulic mortars with addition of high-oleic acid oils in 13 wt.% (FLO13 and HLO13). Large spherical pores play a key role in hampering crack developments during long curing times [69]. Generally, SOM inspections of the pores indicate that the spherical pores range in radius up to ca. 150 μm and their origin are air voids, whereas the convoluted pores are actual cracks caused by shrinkage of the mortars during their setting period [60]. This can provide another explanation for FLO13 and HLO13 mortars to show superior mechanical properties among oiled mortars, as they do not exhibit hair cracks in their sections.

Dynamic elastic modulus exhibits the same trend of compressive strength, showing values in the range of 2.3-8 GPa.

The alterations in mechanical properties of the oiled mortars might be ascribable to a decrease in internal cohesion between oiled aggregates and the binders, as it can be also noted in the fracture surfaces in the SOM micrographs (Figure 34). In these images, the gleaming appearances of the oiled surfaces of the aggregates are evident (especially in cases of oiled AL mortars), which devitalized their adhesiveness to their relative surrounding binders. Nevertheless, as exceptions and in promising accordance with compressive strength results, addition of higher amounts of high-oleic acid oil in mortars with hydraulic properties (FLO13 and HLO13 mortars) increases their elastic modulus after 180 days of curing with respect to non-oiled FL and

HL mortars. Moreover, ALO13showed the lowest reduction in elastic modulus among the investigated oiled AL mortars. The mortars with inclusion of high-oleic acid oils in 13 wt.% previously exhibited substantial decreases in their pores with radius greater than 0.5 μm when compared to their non-oiled references (Figures 28-30).

However, it has to be considered that the hydric and microstructural effects of additive oils have to be evaluated separately. In comparison of high-oleic acid oils and high-linoleic ones, the former one exhibited superior enhancement in microstructure and mechanical properties of the mortars; the latter one demonstrated superior water repellency.

2.3.6 Surface wettability

The additive oils exhibited a significant effect on hydrophobicity of the mortars. These effects were additionally assessed by measuring the surface contact angle (θ). The low contact angle values indicate that the liquid spreads on the surface, while high contact angle values show poor spreading. If contact angle is greater than 90°, the surface is said to be non-wetting with that liquid; surfaces with $0° < \theta < 90°$ are known as wetting surfaces and surfaces with $\theta = 0°$ refer to complete wetting surfaces [94].

As shown in Figure 35, the non-oiled mortars demonstrated complete wetting surfaces; the mortars containing smaller amounts of oils (1.5 wt. %) exhibited wetting surfaces (θ =0-90°), while all sets of mortars containing higher oil contents (13 wt. %) presented non-wetting surfaces (θ=0-90°). The precise surface contact angles of mortars added with 13 wt. % high-oleic acid oil, which previously demonstrated enhanced pore microstructure and mechanical properties, was measured by theta optical tensiometer on a set of

non-wetting (containing 13 wt. % additive oils) air lime, formulated lime and hydraulic lime mortars (Table 8).

The results of surface wettability of the samples were promising, considering that the ordinary lime and cement mortars have wetting surfaces, and the limestone sand and hydrophobic cement mortars (hydrophobised by chemical agents) have initial contact angles of 14.5° and 87° [95], respectively. As reported in Table 8, the highest hydrophobic property in highly oiled mortars was observed in the hydraulic lime (surface contact angle=133.6°). In formulated limes and air limes, this angle was 5° and 10° smaller, respectively.

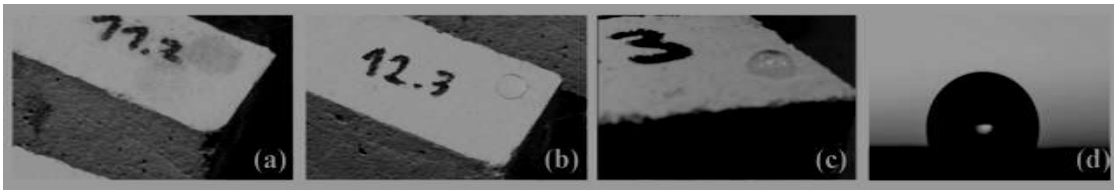

Fig. 35. Wettability of the investigated formulated lime mortars with high-oleic acid oil addition: (a) non-oiled FL mortar; (b) FLO1.5; (c) FLO13; (d) FLO13 by optical tensiometer

Table 8. Surface contact angle of the investigated samples

Sample	Surface contact angle (°)
ALO13	122.5 ± 2.1
FLO13	128.7 ± 5.7
HLO13	133.6 ± 2.5

2.3.7 Freezing-thawing cycles

Durability of the mortars is a demanding property for outdoor rendering materials, thus it was assessed at mortars surfaces by freezing–thawing cycles. The degree of deterioration based on qualitative alterations of the mortars after passing 10 freezing–thawing cycles is reported in Table 9. All the non-oiled

mortars exhibited slight superficial detachments after 5 cycles. The retained water inside hydrophilic pores led to defects and cracks on the surface of the non-oiled material. According to the highest capillary coefficient (Figure 31), the surface of non-oiled HL mortar was further altered and worsened after 10 cycles, with increased superficial cracks and small fractures on its surface.

All the oiled samples did not display any alteration after 10 cycles thanks to their hydrophobic cavities which strongly decrease their capillary coefficients and enhance the durability of the mortars. Literature confirms the positive effects of hydrophobic cavities in lime mortars on their durability and reliability [101].

Table 9. Surface durability of the mortars based on qualitative evaluation after different freezing-thawing cycles

	Qualitative alteration degree		
	2 cycles	5 cycles	10 cycles
AL	0	1	1
ALO1.5	0	0	0
ALQ1.5	0	0	0
ALO13	0	0	0
ALQ13	0	0	0
FL	0	1	1
FLO1.5	0	0	0
FLQ1.5	0	0	0
FLO13	0	0	0
FLQ13	0	0	0
HL	0	1	2
HLO1.5	0	0	0
HLQ1.5	0	0	0
HLO13	0	0	0
HLQ13	0	0	0

Degradation equivalences: 0: without alteration; 1: slight surface detachments; 2: high degree of surface detachments and formation of superficial cracks

2.4 PRELIMINARY EVALUATION OF COMPATIBILITY AS RENDERING MATERIALS

In any case, in terms of total open porosity, all the mortars have values which are commonly considered compatible with historical masonries; TOP in the range of 30-45 % for AL mortars and 18-40 % for hydraulic lime mortars can meet the requirements for restoration of old/historical buildings [4,20] Lower porosity values from this range leads to increment of compactness and impermeability; this can cause condensation of water between the restorative render and the original substrate and lead to very negative consequences. Moreover, too high stiffness emanating from high compactness is not recommended as it can damage the original covered masonry [61].

For rendering old/historical substrates mortars with high stiffness are not favorable materials. The substrate historical masonries exhibit some degree of movement emanating from creep or thermal effects. A mortar that covers them as a rendering mortar should be capable of accommodating movement [61]. Therefore, a rendering material for repair issues with too high stiffness restrains those movements and finally leads to additional stress that can cause failure in the original masonry [102]. This is one of the properties of lime-based mortars that has made them proper as conventional restorative materials; however their designated additives should not worsen their mechanical properties.

Considering the hydrophobic behavior of the oiled mortars in capillarity measurements and despite their slight decrease in permeability values, the hydric properties of the oiled mortars for some special restorative applications can be considered improved with respect to the non-oiled mortars.

The mortar samples were examined after 28 months of curing and no biological alteration was found; however further durability characterizations can assess the potentials of such materials for restoration of built environment.

2.5 CONCLUSIONS (PHASE 2)

The results of this study that aimed to evaluate the hydrophobicity of lime mortars with addition of spent cooking oils and to assess their suitability as restorative rendering materials are depicted as follows:

- The inclusion of additive spent oils increased open porosity and impermeability values and decelerated carbonation rates and workability of the mortars. Generally, these decreases were more evident in higher extent of oils additions. Nevertheless, in terms of open porosity and permeability all of the synthesized mortars remained in ranges which are commonly considered compatible for restorative mortars.
- Only the hydrophilic pores (cavities of non-oiled mortars) exhibit a strong role in water intakes through capillarity**.**
- The addition of spent cooking oils in the lime mortars exhibited a significant hydrophobic effect through capillary phenomenon (reduction from 30 to 60 times) due to hydrophobicity of their vertical tunnels of pores. The additive spent oils, especially high-linoleic acid oil, turned the hydrophilic cavities into hydrophobic ones thanks to their non-polar carbon-hydrogen bonds.
- Addition of oils generally did not enhance the mechanical properties of the mortars due to lowering their rates of carbonation/hydration and hardening. However, addition of higher extent of high-oleic acid spent

cooking oil in the lime mortars brought good hydrophobic added values and did not worsen their mechanical strengths values. Hence, high-oleic acid oils potentially appear as optimum additives for restorative lime mortars.

- Considering the hydrophobic behavior of the oiled mortars in capillarity measurements, their hydric properties can be considered improved with respect to non-oiled mortars, despite their slight decrease in permeability values. 1.5 wt.% oils additions caused an adequate decrease in capillarity and a lower increment of permeability with respect to 13 wt.% oils inclusions.
- Comparing high-oleic (monounsaturated) acid spent cooking oil and high-linoleic (polyunsaturated) one, the former one exhibited superior enhancement in microstructure and mechanical properties of the mortars; the latter one demonstrated superior water repellency.
- The acquired hydrophobicity of the oiled mortars exhibited an increase in their durability and enhancements in their behaviour in facing water and water vapour.

PHASE 3

PARALLEL VALORIZATION OF ORGANICS IN WASTE-BASED RESTORATIVE LIME MORTARS: ALBUMEN + SPENT COOKING OILS AS ADDITIVES

3.1 BACKGROUND AND RESEARCH AIM

Many organic or synthetic additives that enhance certain properties of mortars usually worsen some other characteristics and it has to be considered in their desired applications. As discussed in the second phase of this dissertation, oils additions has on hydrophobicity and durability of the materials; however they generally worsened the microstructure and mechanical properties of the mortars [64,69]. The following study in the third phase assesses the modifications of mortars in presence of proteins and fatty additives, simultaneously. The aim is to assess if the probable improvement of setting rate in presence of added protein, and potential enhancement of hydric properties in presence of oils can be observed in parallel addition of both additives. The suitability of the mortars with parallel valorization of organic waste additives is discussed as potential restorative rendering mortars.

3.2 EXPERIMENTAL PART

3.2.1 Materials

The lime putty used to synthesize the mortars in this study phase is a product described and used in the second phase of this dissertation (§2.2). Discarded commercial bricks (from Wienerberger S.p.A., Terni, Italy) were pulverized with a method used in a previous phase (§2.2). Through laser granulometry (Malvern Instrument) grain size distribution of the pulverized brick waste was determined and demonstrated particle size of ≈10 µm. Chemical composition of pulverized brick determined by ICP plasma, exhibited high oxides percentages of SiO_2 (56 %), CaO (11.22 %), and Al_2O_3 (17.03 %). Quartz was the major crystalline phase of brick waste powder due to XRD analysis. Albite, maghemite, and calcite are other crystalline phases of brick dust. The amorphous content of the pulverized brick was found to be only ~7.7 % as assessed by Rietveld refinement on a Bruker D8 Advance X-ray diffractometer.

High-oleic sunflower spent cooking oil with natural additive antioxidant was prepared as discussed in the second phase (§2.1). The oil was added to the mixes at 1.5 wt.% according to the optimum levels suggested by literature [69]. The used spent cooking oil contained higher percentage of oleic acid (85.42 $\pm$ 0.02) and lower percentage of linoleic acid (5.39 $\pm$ 0.01).

The additive albumen was commercialized product obtained from shelled eggs of barn raised hens. The product was pasteurized and refrigerated albumen (commercialized by Le Naturelle, Italy) and was used in the mortars in 1.5 wt.%. The additive albumen contained 10.1 wt.% protein content.

3.2.2 Samples preparation

The mortars preparation consists in 2 main sets of air lime mortars and lime mortars with hydraulic properties. The abbreviated sample names indicate the

type of binder; L for lime only mortars, BL for lime mortars formulated with brick waste powder, O for spent cooking oil addition and A for albumen inclusion. In synthesis of mortars with hydraulic properties, the addition of an amount of kneading water was necessary to keep their water/binder ratio equal to the air lime mortars. The mix design of the 8 prepared formulations is reported in Table 10.

Table 10. Mix design of the investigated samples

Sample	$Ca(OH)_2$	Pulverized brick	Sand	Added water	Additive spent oil	Additive albumen	Binder/ aggregate ratio
	[wt. %]	[wt. %]	[wt. %]	[wt. %]	[wt. %]	[wt. %]	
L	25.0	-	75.0	-			1:3
LO	23.5	-	75.0	-	1.5	-	1:3
LA	23.5	-	75.0	-	-	1.5	1:3
LOA	22.0	-	75.0	-	1.5	1.5	1:3
BL	19.0	3.0	75.0	3.0	-	-	1:3
BLO	17.5	3.0	75.0	3.0	1.5	-	1:3
BLA	17.5	3.0	75.0	3.0	-	1.5	1:3
BLOA	17.0	2.5	75.0	2.5	1.5	1.5	1:3

A Hobart mortar mixer was used to prepare mortar samples at its low speed. Aggregates and lime putty were mixed for 2 minutes and after 20 seconds pause, the mixture was blended for additional 2 minutes to prepare reference mortar (L). Regarding the synthesis of mortars with hydraulic properties, lime putty, brick waste, aggregates and water were mixed in the automatic mixer for 4 minutes.

Spent cooking oil/albumen added to both mortar types as follows in order to effectively increase the homogenization of the mixes: the organic additive and a minor portion of lime putty were manually blended in a plastic beaker for 2 minutes; then this blended amount was added to the rest of the mix in the Hobart mixer and was mixed for 4 minutes. The sound dispersion of organic

additives in the mixtures was checked and verified visually. No color alteration was observed by naked eye in inclusion of either albumen or spent cooking oil.

The mortars were molded in cubic steel casts (40 x 40 x 40 mm) for dynamic elastic modulus and compressive strength tests, (40 x 40 x 20 mm) for water absorption and (40 x 40 x 10 mm) for surface wettability and capillarity measurement, disc-shaped plastic molds (diameter = 60 mm, thickness = 20 mm) over a thick glass support for permeability and durability assessments, and in cylindrical plastic molds (diameter=30mm, height=50mm) for calcium carbonate determination and porosity (MIP) measurements. In order to accelerate the initial setting of molded mortars, they were positioned inside a basin (T=22 ± 2 °C, RH=98± 2 %) for 6 days and then demolded. The mortars containing pulverized brick were cured in the same condition for their whole curing course (240 days). The air lime mortars were cured naturally in conditioned lab (T=22 ± 2 °C and RH=50±5 %) for 240 days. A schematic illustration of the mortars synthesis is reported in Appendix C.

3.2.3 Samples characterizations

Consistency and setting time. The fresh mortars before their casting were assessed in terms of workability (as was explained in §2.2.3) and setting time according to ASTM C191 [103]. The workability values are averages of two measurements.

Calcium carbonate formation. The calcium carbonate formation rates were assessed as was explained in §2.2.3 at ages of 60, 120, 180, and 240 days of curing. The test specimens were taken from surface of cylindrical samples. The reported values are averages of two measurements.

Pore size distribution. Open porosity measurements were carried out by mercury intrusion porosimeter (MIP) at ages of 60, 120, 180 and 240 days of curing, as was explained in §1.2.3.

Hydric properties. The hydric behavior of lime mortars towards surface water absorptions were investigated in terms of capillarity and surface wettability at age of 120 days of curing on cuboid samples with width of 10 mm. Capillarity measurements were performed according to EN 10859 [104] and surface wettability assessments were carried out by contact sponge method according to UNI 11432 [105]. The reported values are averages of three measurements. Water absorption (WA) was measured on three cuboid samples for each formulation at ages of 120, 180, and 240 days with same method of a first phase of this dissertation (**§**1.2.3). The reported values are averages of three measurements.

Fig. 36. Capillarity measurements

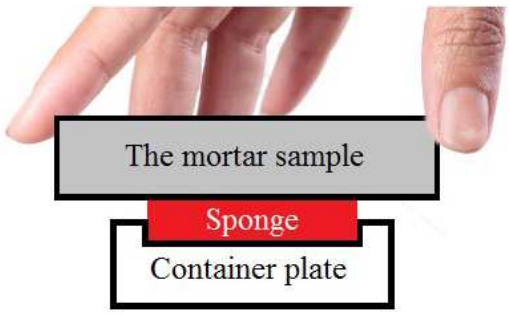

Fig. 37. Schematic drawing of surface wettability test by contact sponge

Water vapor permeability. Water vapor permeability measurements were carried out after 240 days of curing on 3 disc-shaped samples of each formula as was explained in **§**1.2.3. The reported values are averages of three measurements.

Mechanical properties. Measurement of compressive strength was performed as was explained in **§**2.2.3; the results are averages of three measurements on cubic samples (40 × 40 × 40 mm) after 120 and 240 days of curing. Dynamic elastic modulus test (Young's modulus determination) was performed on cubic samples (40 × 40 × 40 mm) at ages of 60, 120, 180 and 240 days of curing as was explained in **§**2.2.3.

Microstructural analysis. Scanning electron and optical microscopies were carried out on the fracture surfaces of the mortars at ages of 120 and 180 days of curing, respectively to investigate their microstructure. The SOM images were collected at 25x magnifications, as was explained in **§**1.2.3. For the SEM analysis the samples were coated with graphite to make them conductive.

Surface freeze-thaw resistance. In order to test the surface durability of the mortars as outdoor rendering materials, 3 cuboid specimens (40 x 40 x 20 mm) for each formulation were subjected to 10 freezing-thawing cycles after 240 days of curing. The specimens were immersed in water for 30 mins, then placed on a plastic drain in conditioned lab (T=22 ± 2 °C and RH=50±5) for 30 minutes in order to provide them the opportunity to discharge their potential gained water, and then positioned in lab freezer at −20 ±2 °C for 3 hours. The selected cycle was aimed to simulate a destructive circumstance in a cold environment when the trapped water inside cavities freezes and leads to frost damage due to ice volume expansion. Assessment of the mortars suitability for outdoor rendering was based on qualitative alteration investigations.

3.3 RESULTS AND DISCUSSION

3.3.1 Fresh states

3.3.1.1 Workability

Workability values of the fresh mortars are reported in Figure 38. The parallel addition of pulverized brick and added kneading water did not alter the consistency of the mortars. Addition of either spent cooking oils or albumen caused a decrease in the workability values. The early physical effects of albumen additions in mortars were similar to oils additions. These organic additives increase the internal cohesion of the mortars due to covering the aggregates and solid particles of the binder and turning them into less workable materials. In case of quantitative increments of these viscous organic additions, the lowest workability among air lime mortars was observed (LOA and BLOA).

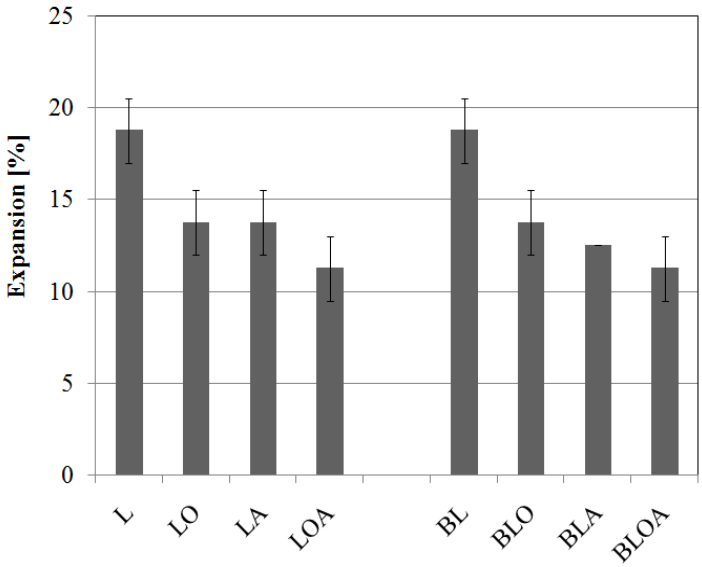

Fig. 38. Workability of the investigated mortars

3.3.1.2 Setting time

Initial and final setting times of the fresh mortars are reported in Figure 39. L and BL sample demonstrated comparable initial setting time; however brick powder addition caused few hours of retarding in the final setting time. Also addition of spent cooking oils (LO and BLO) retarded the setting times, probably due to reduction of carbon dioxide gain through oiled surfaces that led to lowering carbonation and setting rates. Addition of albumen significantly decreased the setting times of the mortars from both categories of air limes and formulated limes. Unlike to fatty acids, most of proteins have amphiphilic surfaces. They usually have their hydrophobic parts buried within their core and their hydrophilic residues facing outside [106]. When proteins are added to the lime mortar, they become unfolded under high pH and their hydrophobic parts face outside. The modified proteins congregate near the superficial layer of the mortars and cause an uneven distribution of matters and consequently ion concentration gradient. This leads to an increment in evaporation rate of water in mortar and eventually acceleration of curing and setting [9]. The parallel addition of spent cooking oils in lime-albumen mortars did not compromise on their setting rate.

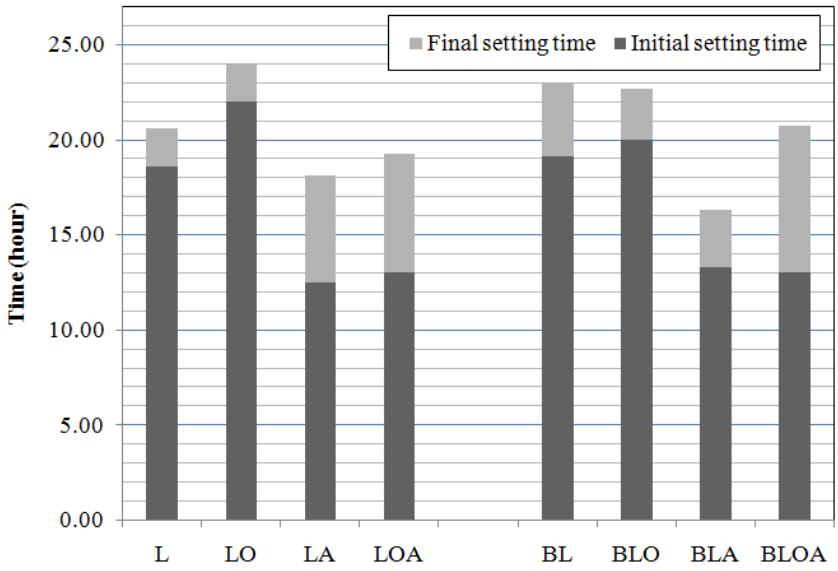

Fig. 39. Initial and final setting times of the fresh mortars

3.3.2 Hardened state results

The mortars are characterized at the ages of 60, 120, 180 and 240 days. Table 11 shows the values of open porosity (MIP) at 240 days of curing, dry density, water absorption, capillarity coefficient, surface wettability and compressive strength of the mortars assessed after 120 days of curing. Generally, addition of organics increases the open porosity values and formations of air voids. This effect could be clearly observed by the formed air bubbles on the water surface when the mortars were immersed in water for the water absorption tests. The MIP assessments in curing ages earlier than 240 days sometimes showed lower total open porosity values, while the dry densities did not demonstrate increments as a factor of curing time. Hence, in higher curing ages some air macro pores that are out of MIP detection range (60 microns) might be cured and enter this range and register a higher open porosity value.

Table 11. Physical and mechanical properties of the investigated mortars: open porosity (MIP) at age of 240 d; dry density, water absorption, capillarity coefficient, surface durability, and compressive strength of the mortars assessed after 120 d of curing. The values correspond to the average (±standard deviation)

Mortar	Open porosity with MIP (%)	Dry density (g/cm3)	WA (%)	Capillarity coefficient (mg/cm2.√s)	Surface wettability (kg/cm2.S)	Compressive strength (MPa)
L	26.44	1.9 (± 0.0)	9.4 (± 0.1)	7.3 (± 0.1)	0.18 (± 0.02)	1.4 (± 0.4)
LO	31.18	1.8 (± 0.0)	2.1 (± 0.1)	0.3 (± 0.0)	0.01 (± 0.00)	0.4 (± 0.4)
LA	34.92	1.9 (± 0.0)	8.5 (± 1.2)	6.9 (± 0.2)	0.20 (± 0.04)	1.3 (± 0.1)
LOA	32.52	1.7 (± 0.0)	3.1 (± 0.2)	0.3 (± 0.1)	0.02 (± 0.00)	0.5 (± 0.0)
BL	34.86	1.8 (± 0.0)	10.1 (± 0.1)	7.0 (± 0.2)	0.12 (± 0.03)	1.0 (± 0.3)
BLO	38.46	1.8 (± 0.0)	2.5 (± 0.2)	0.3 (± 0.0)	0.01 (± 0.00)	1.5 (± 0.1)
BLA	34.92	1.7 (± 0.0)	10.6 (± 0.1)	5.6 (± 0.4)	0.10 (± 0.03)	0.3 (± 0.0)
BLOA	31.85	1.8 (± 0.0)	3.1 (± 0.4)	0.5 (± 0.0)	0.01 (± 0.00)	0.4 (± 0.1)

Formulating the mortars with pulverized brick-waste did not generally enhance their hydric properties. Literature reports high reduction of water absorption with inclusion of amorphous pozzolanic materials such as metakaolin [67]; as previously mentioned the amorphous content of the used brick dust is very low (~7.7 %) and hence not very reactive in forming CSH phases with respect to amorphous pozzolanic additives. However, the contribution of open porosity of mortars in their capillarity and water gains can be basically related only to hydrophilic cavities.

Substantially high water absorption values and capillarity coefficients are registered for the non-oiled mortars as they possess hydrophilic pores where water can easily enter and move vertically [90]. These water absorption values demonstrated a considerable decrease when oil was added to the mixes. Comparing these reductions with the literature, capillarity reduction of the air lime mortars with high-oleic spent cooking oils is much lower than the same amount of linseed oil addition by Nunes [67] (24% instead of 56% reduction). This is because of higher reactivity and unsaturation of linseed oil with respect to the oil used in this study. Higher unsaturation level allows the carboxyl

groups of the fatty acids to have higher reaction with the oxygen of the air and other carboxyl groups. All facilitates the fatty acids to coordinate with the present lime and being trapped inside the binder to create water repellency thanks to hydrophobic parts of the molecules [63,67,91]. However, addition of spent mono-unsaturated fat oils as hydrophobic agents substantially decreased the surface wettability and water absorption values. In oiled mortars, the internal surfaces of cavities coated with layers of fatty materials turned their hydrophilic properties of into hydrophobic ones. Generally, as previously discussed, in organic protein-lime mortars the modified proteins under high pH congregated near the mortar surface and slightly improve the superficial water resistances [9]. This property changes the states of cavities of lime mortars from hydrophilic to amphipatic and slightly decreases the water gains of albumen-lime mortars. However, air lime-albumen mortar (LA) did not show a reduction in surface wettability with respect to its reference. The high porosity of LA mortar facilitated its water gain from saturated sponge. Pore size distribution graph of the mortars (Figures 40 and 41) demonstrate a considerable extent of capillarity pores dedicated to LA and BLA mortars. Moreover, the increment of air voids in lime-albumen mortars, with respect to their references is visible in SOM images in Figure 42; these pores compensate the discussed amphipatic property of albumen additions in facing water. In SOM images better aggregate-binder bonding seems to be appeared in brick-lime mortars.

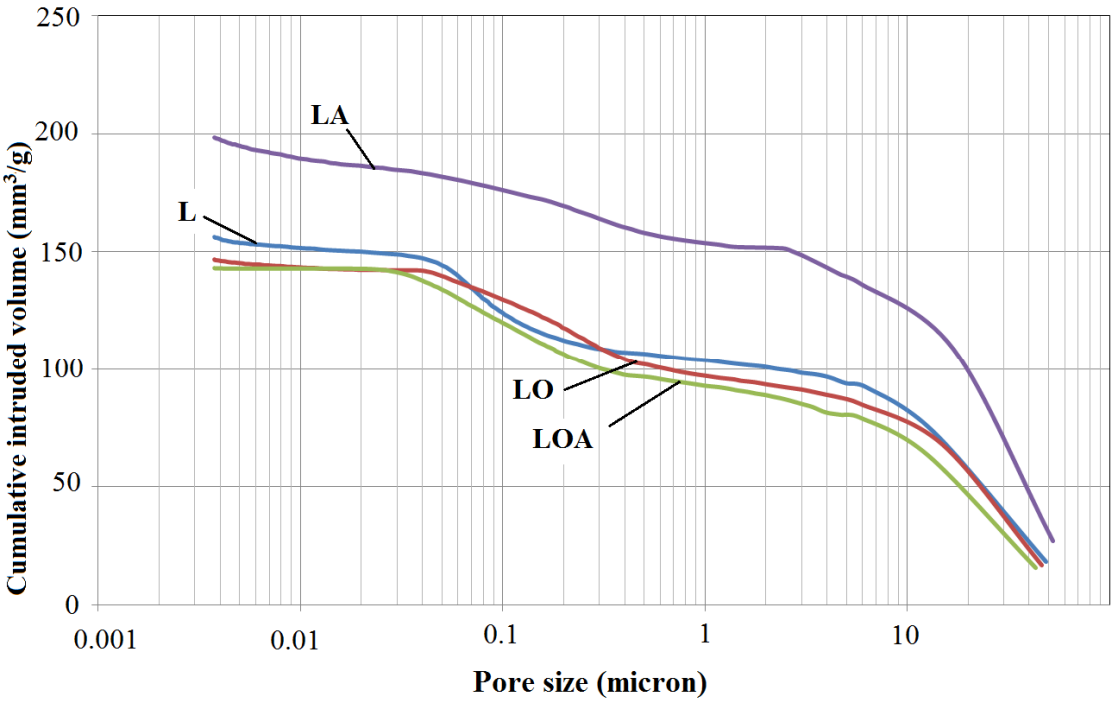

Fig. 40. Pore size distribution of air lime mortars at 240 days of curing

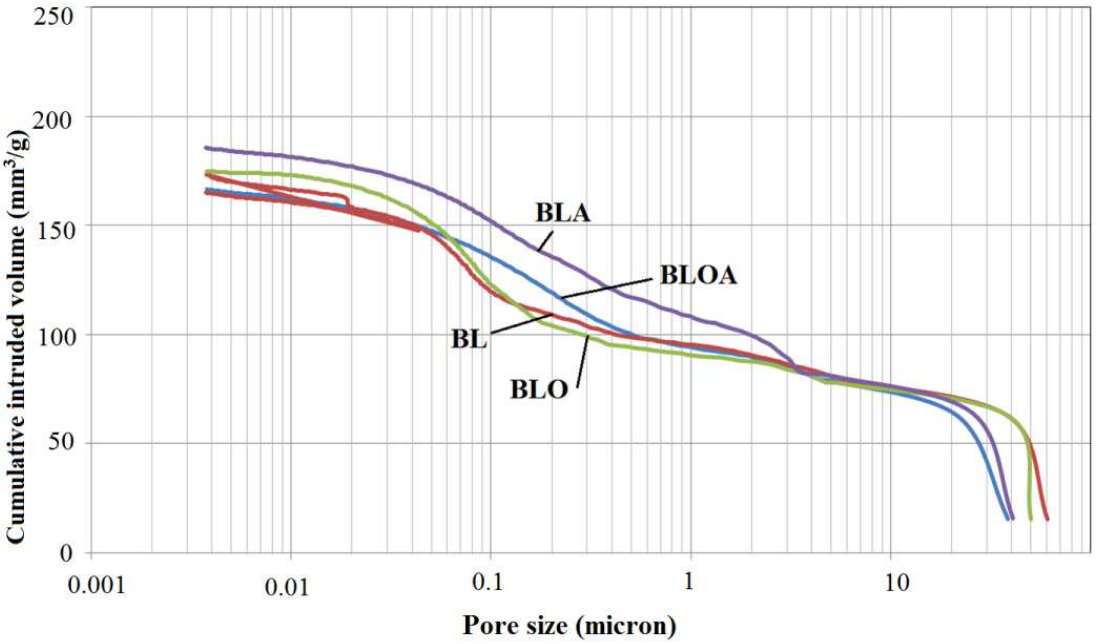

Fig. 41. Pore size distribution of formulated lime mortars at 240 days of curing

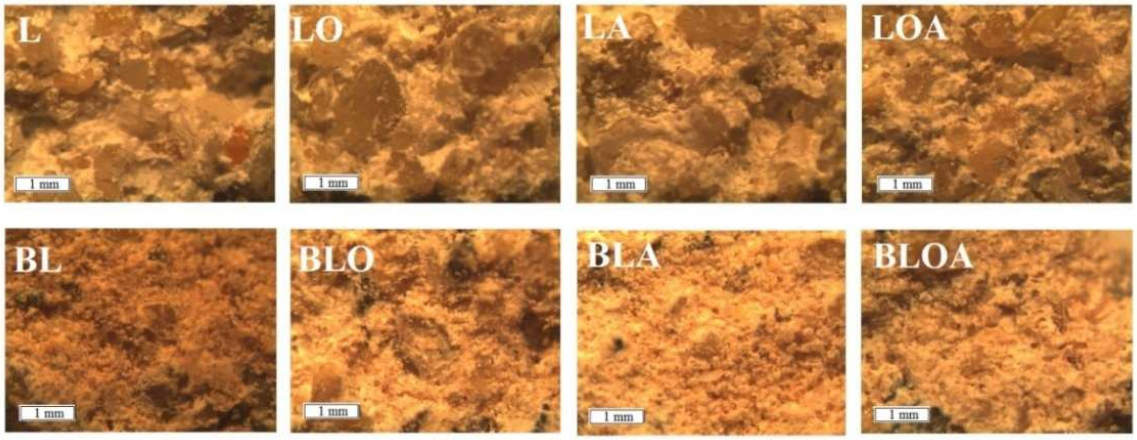

Fig. 42. SOM micrographs of the fracture surfaces of the samples at 180 days of curing

Water absorption values of the mortars at different curing ages are reported in Figure 43. As previously discussed, mortars showed considerable water absorption reductions with addition of oils, either with or without albumen. This positively means that LOA and BLOA samples made profit of protein additions (i.e. accelerated setting) and were hydrophobized by fatty acids, in a parallel addition. The water resistance of the mortars generally exhibited improvements as a factor of curing time. Completion calcium carbonate formation through carbonation and/or hydration leads to slow enhancements in the microstructures and consequently water absorption reductions through natural aging process.

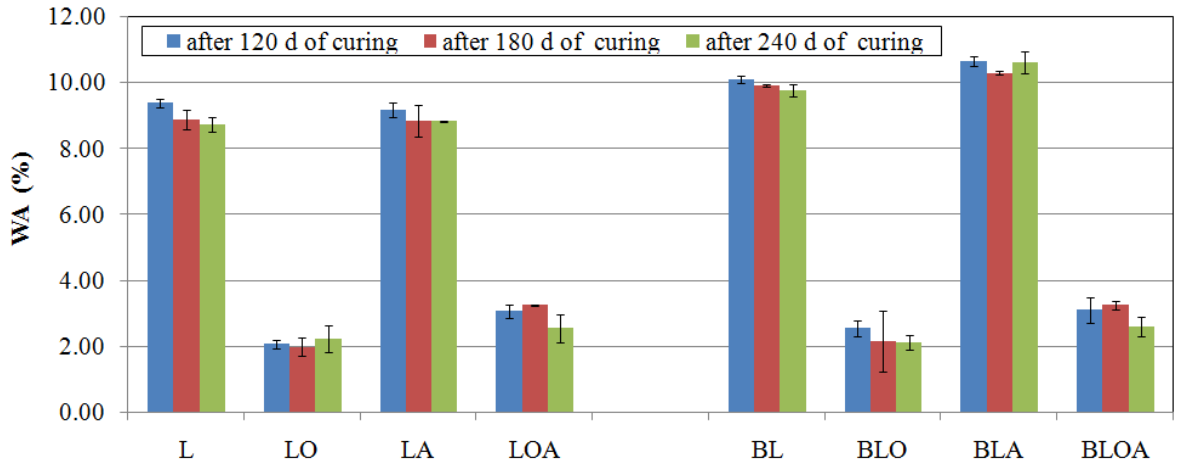

Fig. 43. Water absorption of the mortars after 120, 180 and 240 days of curing

Calcium carbonate formations on surfaces of the mortars were studied after 60, 120, 180 and 240 days of curing as reported in Figure 44. For brick-lime mortars the reported calcium carbonate content due to the brick powder (ca. 2.28 % by calcimetry measurement) is subtracted from $CaCO_3$ contents of mortars; hence, the reported calcium carbonate content deals with carbonation/hydration of calcium hydroxide.

The surfaces of non-oiled L mortar exhibited 98% of its carbonation in the first 60 days of curing. For all of the air lime mortars, the carbonation process ceased before the age of 180 days as they did not exhibit extra $CaCO_3$ formation in monitoring up to age of 240 days. In case of mortars formulated with brick powder, calcium carbonate formation accelerated after age of 60 days due to low setting rate through hydration reactions. This is due to essentially slower hydration process for formation of calcium carbonate in lime mortars with hydraulic properties than the carbonation procedure in air lime mortars. Moreover, pozzolanic reaction between pulverized brick and $Ca(OH)_2$ limits carbon dioxide gain and reduces the lime amount capable for carbonation.

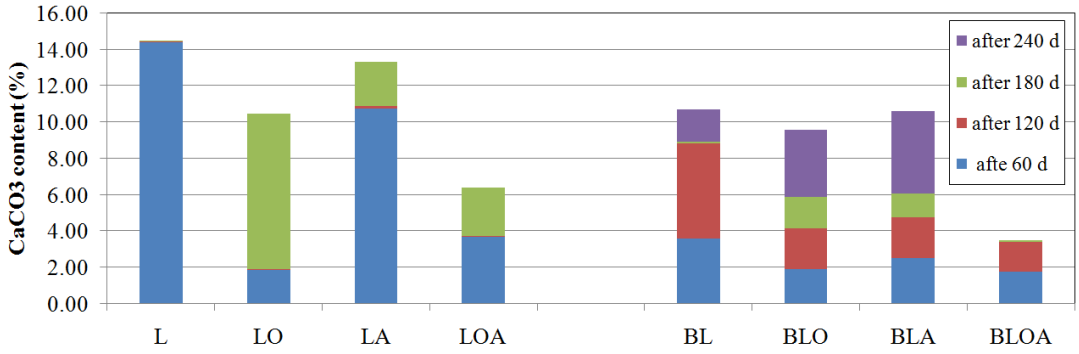

Fig. 44. Calcium carbonate formation of limes at the surfaces of mortars after 60, 120,180 and 240 days of curing

After 240 days of curing the same trends of calcium carbonate formation were observed in both cases of air lime and formulated lime mortars. The addition of spent cooking oil decelerated the carbonation rates in air lime mortars, probably due to hindering their CO_2 gain necessary for carbonation. Addition of albumen to mortars increased their carbonation rate due to previously discussed uneven distribution of matters and ion concentration gradient caused by unfolded proteins in the alkaline ambient. However, parallel addition of albumen and oil, negatively resulted in reduction of carbonation rate at mortars surfaces probably due to increment of the superficial hydrophobicity of the mortars. The samples for carbonation assessments were obtained from surfaces of the mortars, where in parallel case of albumen and oil addition, probably contains high concentration of amphipatic (from coagulated unfolded proteins at surfaces) and hydrophobic fragments. Hence, LOA and BLOA exhibited low calcium carbonate formation at their surfaces, which does not necessarily induce concluding high impermeability for these materials.

Water vapor impermeability (or water vapor resistance) values of the mortars ranged between 7 and 11.5 and are reported in Figure 45. Permeability for restorative rendering materials is generally counted as a very promising value as facilitates draining the humidity inside masonries . Addition of albumen increased the permeability of the mortars due to open porosity increments. Addition of oil had a different effect on permeability of air lime and brick-lime mortars; in former cases it increased the impermeability and in the latter one it increased the permeability values. Impermeability can be considered as a factor of microstructure densification; parallel additions of albumen and oil exhibited high impermeability values among brick-limes as a result of possession of dense microstructure (Table 11 and Figures 40 and 41). In case of air lime mortars parallel additions of the organics, increased their permeability as a result of increment of open porosity values. However, "renovation mortars" can have an impermeability value lower than 15 [94] hence slight permeability reductions do not compromise on their suitability as restorative rendering materials. The different behavior of oil addition in air limes and brick-limes can be discussed in terms of microstructural alterations in presence of these organics.

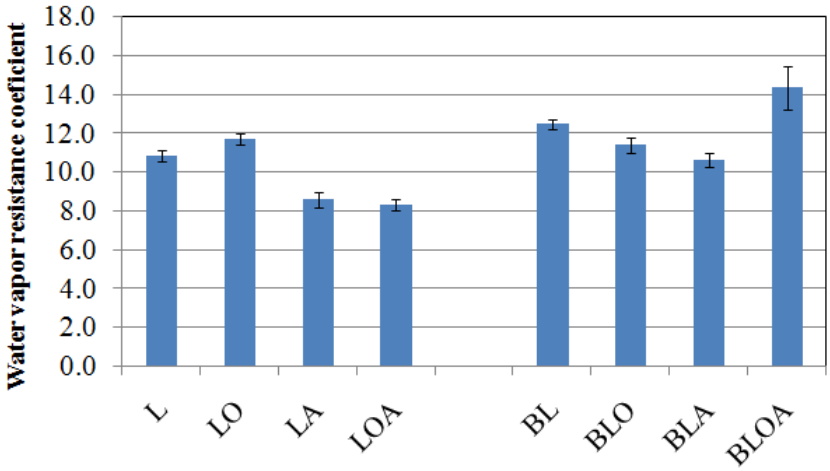

Fig. 45. Resistance to water vapor diffusion of the investigated samples at 180 days of curing

As assessed by SEM/EDS (Figures 46 and 47) growth of fiber and flake crystals in oiled brick-lime mortars led to improve their microstructural consistency. Also as reported elsewhere [67] the carboxyl acid derivates have the capability to change morphology of mortars with lime and pozzolanic hydrated phases but not air limes; oils additions had weakened the microstructure and compressive strength of LO mortar and improved them in case of BLO mortar. In cases of either oil or albumen additions, the morphology alterations microstructure of formulated mortars with brick dust can be more evident than alterations in air lime mortars as the concentration of fatty acids and albumen are higher with respect to air limes due to consumption of water by pulverized brick. Hence, organic phases are more visible in BLA mortar than LA sample; albumen-air lime mortars demonstrated compact structures. Generally addition of oils either as a single additive or parallel with albumen, formed sizable crystals and less compact structures. This can be ascribed to formation of pores during mixing organic additives that creates bigger spaces and potentials for larger crystals growths [67] that happened also in parallel additions of oils and albumen. The binders of LOA and BLOA samples in low magnifications (Figure 47) seemed to demonstrate low internal cohesion and bonding that could highly affect their mechanical properties of the mortars.

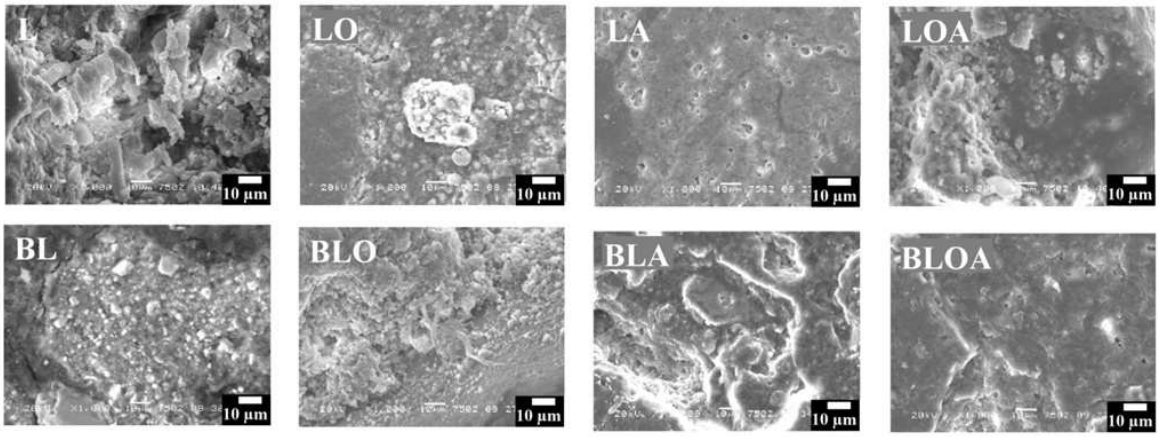

Fig. 46. SEM micrographs of the mortars samples (secondary electrons, 1000× magnification)

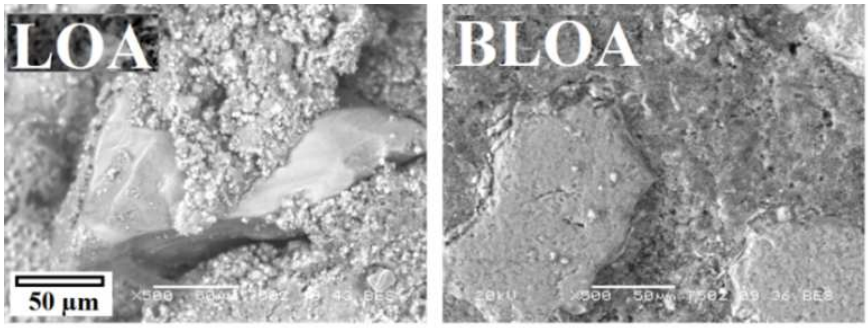

Fig. 47. SEM micrographs of parallel added air lime mortar sample (left) brick-lime mortar (right) (back scattered electrons, 500× magnification)

The mechanical properties of the mortars reported in Table 11, showed an increments through natural curing at age of 240 days as the results of compressive strength (Figure 48) and dynamic elastic modulus are reported (Figure 49). The microstructure of the BLO mortar demonstrated high growth of fiber and flake crystals and a good compressive strength. Nevertheless, inclusion of oil in parallel addition with albumen did not enhance the mechanical properties of brick-lime mortars. A reason can be found in SOM micrographs of fracture samples (Figure 42); BLO mortar showed well distributed spherical pores (~0.3 mm diameter) probably with origin of air voids. In BLOA mortar however, the convoluted pores are sections of actual

hair cracks probably caused by shrinkage of the mortars during their curing period [60]. Presence of internal hair cracks can be another reason for parallel organic added mortars to demonstrate low dynamic elastic modulus (Figure 49) as prolongs the ultrasonic waves transfer.

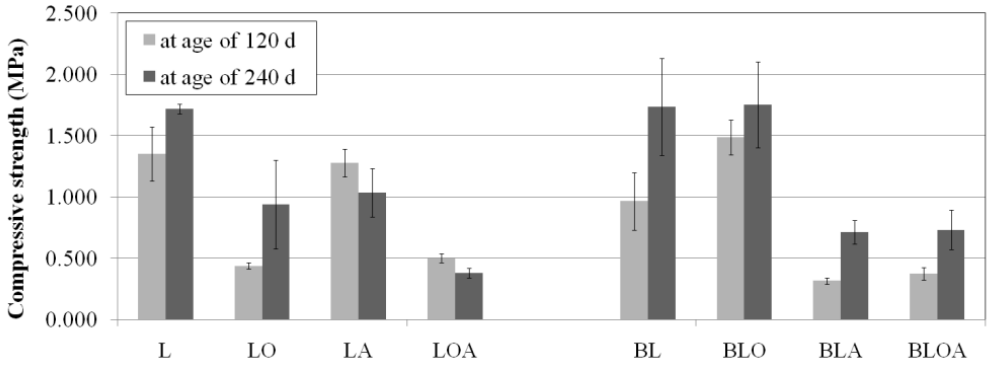

Fig. 48. Compressive strength of the investigated samples at 120 and 240 days of curing

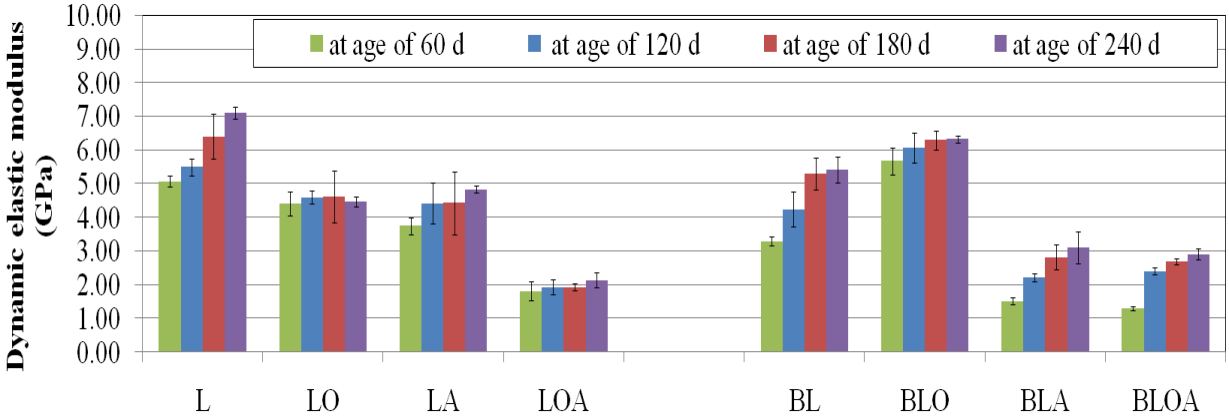

Fig. 49. Dynamic elastic modulus of the samples at 60, 120, 180 and 240 days of curing

For a rendering material to cover old/historical substrates mortars with high stiffness are not favorable materials as they block the movements of the historical/old masonries generated from thermal effects or creep. Therefore, a restorative rendering material with too high stiffness can induce additional stress and eventual failure in the original masonry [61,102]. Hence, modifications of restorative lime mortars are not usually aimed at substantial increments of their mechanical properties as possession of not too high

stiffness is one of the items that has made them proper as repair materials. Addition of oils to lime mortars previously in SEM images showed growth of fiber and flake crystals in oiled brick-lime mortars (Figure 46) led to improve their consistency and mechanical properties. Brick-lime mortars did not cease their carbonation till the age of 240 days (Figure 44) and they consequently showed increments in their compressive strengths through natural curing. Nevertheless, air lime mortars with inclusion of albumen and low carbonation extent after 120 days did not show enhancements in their mechanical properties. Generally, in terms of compressive strength the organic additions exhibited a more promising result in case of formulated mortars rather than air limes. Dynamic elastic modulus monitoring of mortars confirmed their modifications through natural curing (Figure 49).

Surface freeze-thaw resistance of the mortars as an important property for outdoor rendering applications was assessed by freezing–thawing cycles. Through 10 freezing–thawing cycles the degrees of superficial deterioration based on visible-qualitative alterations were assessed. The non-oiled mortar samples showed slight superficial detachments after passing 5 destructive cycles as their hydrophilic cavities retained water and induced defects and cracks on their surfaces due to freezing expansion of ice.

Albumen-lime mortars without oil inclusion did not show the adequate surface durability as they manifested cracks and material loss after 7 cycles. All the oiled samples (including parallel additions with albumen) showed surface soundness after 10 cycles firstly thanks to their low water absorption; secondly their hydrophobic pores induce them to discharge their low amount of gained water before freezing; third high open porosity that developed their frost resistance.

3.4 CONCLUSIONS (PHASE 3)

Addition of spent cooking oils in mortars led to significant hydrophobic effects such as reductions of 75-77 % in water absorption and 95 % in capillarity values. The oiled mortars moreover showed a substantial superior surface durability with respect to their references. Nevertheless, oil additions had negative effects on consistency, permeability and setting time of the mortars. Albumen-only additions in lime mortars enhanced the carbonation rate and setting time of the mortars, but substantially increased the open porosity values and led to reductions in their hydric properties. Parallel valorization of albumen as organic protein source and fatty acid additive demonstrated enhanced setting time and improved hydrophobicity and enhanced durability at the same time, for both air and formulated lime categories. However they exhibited low mechanical properties, they can be suitable for restorative applications without high stiffness requirements. Parallel valorization of organic additions in lime mortars can explore high potentials in designing restorative materials with low environmental impact and high respect to the feature of historic mortars.

FINAL REMARKS

Some binders/mortars with waste-based additives were synthesized, characterized and their suitability for restorative applications was assessed. The waste-based organic and ceramic additives either in alkali-activated binders or new historic lime mortars demonstrated high potentials as precursor/addition in restorative materials.

As the first phase of the dissertation, binders from alkali-activation of brick waste powder were synthesized, characterized and evaluated as possible materials for repointing historic/old masonries. The binders with nominated SiO_2/Al_2O_3 molar ratio ranging from 1.4 to 0.4 in two different curing temperatures (room temperature and 50 °C) were investigated. The open porosity of the binders was found to decrease for decreasing the nominated molar ratio. For SiO_2/Al_2O_3 = 1.4, the molar ratio was suitable for reaching a good geopolymerization level, but enough reactive fractions were available to form a continuous geopolymeric matrix embedding unreacted fractions. Progressive addition of sodium aluminate (causing the SiO_2/Al_2O_3 ratio to decrease down to 0.4) resulted in progressive microstructure densification. The decrease of this molar ratio caused efflorescence, as progressive addition of sodium aluminate induced a higher amount of Al_2O_3 available for geopolymerization and a lower amount of unreacted sodium oxide to form sodium carbonate efflorescences upon carbonation.

Open porosity and efflorescence formation were found to decrease for decreasing SiO_2/Al_2O_3 ratio. Curing at high temperature generally favored

geopolymerization and reduced efflorescences formation. Pastes with SiO_2/Al_2O_3 = 0.8 and 0.9 exhibited open porosity and water vapor permeability falling in the index range of historic lime-based mortars, thus proving to be potentially compatible with them. As for the possible use of pastes from brick waste alkali-activation for repointing historic masonries, among the investigated formulations those with intermediate SiO_2/Al_2O_3 ratios exhibited potential compatibility with historic mortars.

As the second phase of the dissertation, suitability of new lime mortars for restorative rendering applications was investigated. Air-, formulated- and hydraulic-lime mortars were synthesized with inclusion of two different types of spent sunflower cooking oils and, when necessary, brick waste powder as pozzolanic addition. The results of spent cooking oils addition in the mortars exhibited promising hydrophobic effects, such as sorptivity reduction up to 60 times and improvement of superficial durability especially in case of high-linoleic oil addition. Addition of oils generally did not enhance the mechanical properties of the mortars due to lowering their rates of carbonation/hydration and hardening. However, addition of higher extent of high-oleic acid spent cooking oil in the lime mortars brought good hydrophobic added values and did not worsen their mechanical strengths values. Hence, high-oleic acid oils potentially appear as optimum additives for restorative lime mortars. Considering the hydrophobic behavior of the oiled mortars in capillarity measurements, their hydric properties can be considered improved with respect to non-oiled mortars for certain restorative applications, despite their slight decrease in permeability values. Comparing high-oleic (monounsaturated) acid spent cooking oil and high-linoleic (polyunsaturated) one, the former one exhibited superior enhancement in microstructure and mechanical properties of the mortars; the latter one demonstrated superior water repellency. The acquired hydrophobicity of the oiled mortars exhibited an increase in their

durability and enhancements in their behaviour in facing water and water vapour. All the investigated mortars exhibited appropriate indexes as restorative materials.

In the third phase of the dissertation, air- and formulated lime mortars with pulverized brick waste were synthesized with addition of two organic waste-based additives: spent cooking oil and albumen. Addition of spent cooking oils in mortars led to significant hydrophobic effects such as reductions of 75-77 % in water absorption and 95 % in capillarity values. The oiled mortars moreover showed a substantial superior surface durability with respect to their references. However, oil additions had negative effects on consistency, permeability and setting time of the mortars. Albumen-only additions in lime mortars improved the carbonation rate and consequently reduced the setting time of the mortars, however, it substantially increased the open porosity values and led to reductions in their hydric properties. Parallel valorization of albumen as organic protein source and fatty acid additive demonstrated enhanced setting time and improved hydrophobicity and enhanced durability at the same time, for both air and formulated lime categories. However they exhibited low mechanical properties, they can be suitable for restorative applications without high stiffness requirements. Parallel valorization of organic additions in lime mortars can explore high potentials in designing restorative materials with low environmental impact and high respect to the feature of historic mortars.

The modifications of binders and mortars aimed at their hydric enhancements can lead to a superior bonding with substrates. Hydrophobic mortars and their substrates can compete and do not let water be absorbed by support quickly. So the possibility of lime particles filling the cavities of substrates increased. When the mortar is cured, its bond with the base tightly

improved. It also leads to improve the durability and frost resistance of the repair materials.

Improvement of durability and reliability of economically friendly restorative materials with low environmental impact leads to potential for restoration of the built environment. However, these materials need to be furthermore assessed in in-situ applications. In-situ application can be an important transition phase before restorative applications in historical buildings.

Fig. 50. A 20th century house in Masshad (north-eastern Iran) as an example of a national heritage element in need of repointing with sustainable binder

Finding a proper historical element for preliminary in-situ applications in Italy was not feasibly possible; however, many developing countries with rich history of cultural heritage, including Iran have a vast domain of old/ historical buildings in need of modern conservation with sustainable materials. For such countries with numerous 'under restoration' and 'in need of restoration' elements the feasibility of conservation for medium importance index elements of the built environment is tightly related to economical considerations of the

conservation plans. Hence, application of new restorative waste-based materials can decrease the restoration costs and consequently spread the possibilities to treat built environment.

Preliminary exploration of possibilities for in-situ applications of the discussed sustainable waste-based restorative materials in Persian old/historical built environment has been carried out. The Iranian National Cultural Heritage-Handicrafts-Tourism Organization as the responsible authority for conservation of built environment in Iran has agreed to explore the potentials for in-situ application of the new historic mortars by this dissertation.

This set of potential in-situ applications will be a step toward promoting sustainable waste-based restorative mortars which respect the feature of historic mortars and have the microstructures and physical properties similar to the materials that are accepted 'suitable' for restoration of built environment.

REFERENCES

[1] G. Amoroso, V. Fassina, Stone decay and conservation, Material Science Monograph 11, Elsevier, 1983

[2] E. Bertacchini, G. Segre, Introduction: Culture, sustainable development and social quality: A paradigm shift in the economic analysis of cultural production and heritage conservation, City, Culture and Society 7 (2016) 69-70

[3] P. Faria, F.M.A. Henriques, Current mortars in conservation: an overview, Intr Jrnl Restor 6 (2004) 609-622

[4] P. Maravelaki, A. Bakolas, I. Karatasios, V. Kilikoglou, Hydraulic lime mortars for the restoration of historic masonry in Crete, Cement and Concrete Research 35(2005) 1577-1586

[5] L. Ventolà, M. Vendrell, P. Giraldez, L. Merino, Traditional organic additives improve lime mortars: New old materials for restoration and building natural stone fabrics, Constr Build Mater 25(2011) 3313-3318

[6] J. Grilo, P. Faria, R. Veiga, A. Santos Silva, V. Silva, A. Velosa, New natural hydraulic lime mortars: physical and microstructural properties in different curing conditions, Constr Build Mater 54 (2014) 378-384

[7] A. Petrillo, R. Cioffi, F. Felice, F. Colangelo, C. Borrelli, An Environmental Evaluation: A Comparison Between Geopolymer and OPC Concrete Paving Blocks Manufacturing Process in Italy Environmental Progress & Sustainable Energy Volume 35, Issue 6, Version of Record online: 25 JUL 2016

[8] H. Schellnhuber, Global warming. Stop worrying, start panicking? Proceedings of the National Academy of Sciences of the United States of America 105 (2008) 14239– 14240

[9] S. Fang, K. Zhang, H. Zhang, B. Zhang, A study of traditional blood lime mortar for restoration of ancient buildings, Cement and Concrete Research 76 (2015) 232-241

[10] M. Hall., R. Lindsay, M. Krayenhoff, Modern earth buildings (2012) Cambridge: Wood-Head Publishing

[11] F. Pacheco-Torgal, J. Barroso de Aguiar, Y. Dingz, et al., Performance of alkali-activated mortars for the repair and strengthening of OPC concrete, Handbook of alkali-activated cements, mortars and concretes (2015), pp. 627-641

[12] G. Wei, H. Zhang, H. Wang, S. Fang, B. Zhang, F. Yang, An experimental study on application of sticky rice-lime mortar in conservation of the stone tower in the Xiangji Temple, Constr Build Mater 28 (2012) 624-632

[13] F. Beracca, C.R. Fichera, Use of olive stone as an additive in cement lime mortar to improve thermal insulation, Ener Build 62 (2013) 507-513

[14] M. Lanzon, P.A. Garcia-Ruiz, Evaluation of capillary water absorption in rendering mortars made with powdered water proofing additives, Constr Build Mater 23 (2009) 3287-3291

[15] K. Van Balen, I. Papayanni I., R. Van Hees, L. Binda, A. Waldum, Introduction to requirements for and functions and properties of repair mortars, Materials and Structures 38 (2005) 781-785

[16] E. Franzoni, The role of mortars in ancient brick masonries' decay: a study in the Pio Palace at Carpi (Italy), in J. Válek, C. Groot and J.J. Hughes (editors), "2nd Historic Mortars Conference HMC2010 and RILEM TC 203-RHM Final Workshop", 22-24 September 2010, Prague, Czech Republic, 483-490 (CD) (RILEM Proceedings PRO 78)

[17] F. Sandrolini, E. Franzoni, G. Cuppini, L. Caggiati, Materials decay and environmental attack in the Pio Palace at Carpi: a holistic approach for historical architectural surfaces conservation, Building and Environment 42 (2007) 1966-1974

[18] F. Sandrolini, E. Franzoni, Characterization procedure for ancient mortars' restoration: The plasters of the Cavallerizza courtyard in the Ducal Palace in Mantua (Italy), Materials Characterization 61 (2010) 97-104

[19] E. Aggelakopoulou, A. Bakolas, A. Moropoulou, Properties of lime-metakaolin mortars for the restoration of historic masonries, Applied Clay Science 53 (2011) 15-19

[20] A. Moropoulou, A. Bakolas, P. Moundoulas, E. Aggelakopoulou, Anagnostopoulou S., Optimization of compatible restoration mortars for the earthquake protection of Hagia Sophia, Journal of Cultural Heritage 14S (2013) e147-e152

[21] E. Sassoni, P. Pahlavan, E. Franzoni, M.C. Bignozzi, Valorization of brick waste by alkali-activation: A study on the possible use for masonry repointing, Ceram Int 42 (2016) 14685–14694

[22] J. Davidovits, Geopolymers: inorganic polymeric new materials, J Thermal Anal. 37 (1991) 1633–1656. 269 (2005) 47-58

[23] F. Pelisser, E.L. Guerrino, M. Menger, M.D. Michel, et al., Micromechanical characterization of metakaolin-based geopolymers, Construction and Building Materials 49 (2013) 547–553

[24] P. Duxson, A. Fernandez-Jimenez, J.L. Provis, et al., Geopolymer technology: the current state of the art, J Mater Sci 42 (2007) 2917–2933

[25] C. Kuenzel, T.P. Neville, S. Donatello, L. Vandeperre, et al., Influence of metakaolin characteristics on the mechanical properties of geopolymers, Applied Clay Science 83-84 (2013) 308-314

[26] P. Rovnaník, Effect of curing temperature on the development of hard structure of metakaolin-based geopolymer, Construction and Building Materials 24 (2010) 1176–1183

[27] P. Duxson, J.L. Provis, G.C. Luckey, J.S.J Van Deventer, The role of inorganic polymer technology in the development of ‘Green Concrete’, Cem Concr Res, 37 (2007) 1590–1597

[28] F. Pacheco-Torgal, J. Castro-Gomes, S. Jalali, Alkali-activated binders: A review - Part 1. Historical background, terminology, reaction mechanisms and hydration products, Construction and Building Materials 22 (2008) 1305-1314

[29] F. Puertas, I. García-Díaz, A. Barba, M.F. Gazulla, M. Palacios, et al., Ceramic wastes as alternative raw materials for Portland cement clinker production, Cem Concr Compos 30 (2008) 798–805

[30] F. Puertas, I. García-Díaz, M. Palacios, et al., Clinkers and cements obtained from raw mix containing ceramic waste as a raw material characterization, hydration and leaching studies, Cem Concr Compos 32 (2010) 175–186

[31] M.C. Bignozzi, S. Manzi, I. Lancelotti, E. Kamseu, L. Barbieri, C. Leonelli, Mix-design and characterization of alkali activated materials based on metakaolin and ladle slag, Applied Clay Science 73 (2013) 78-85

[32]M.C. Bignozzi, S. Manzi, M.E. Natali, W.A.D. Rickard, A. van Riessen, Room temperature alkali activation of fly ash: The effect of NaO/SiO2 ratio, Construction and Building Materials 69 (2014) 262-270

[33] Z. Sun, H. Cui, H. An, D. Tao, D. Xu, Y. Xu,J. Zhai, Q. Li, Synthesis and thermal behavior of geopolymer-type material from waste ceramic, Construction and Building Materials 49 (2013) 281-287

[34] L. Reig, M.M. Tashima, L. Soriano, M.V. Borrachero, J. Monzò, J. Paya, Alkaline activation of ceramic waste materials, Waste and Biomass Valorization 4 (2013) 729-736

[35] L. Reig, M.M. Tashima, M.V. Borrachero, J. Monzò, Cheeseman C.R. Paya J., Properties and microstructure of alkali-activated red clay brick waste, Construction and Building Materials 43 (2013) 98-106

[36] I. Lancellotti , C. Ponzoni, M.C. Bignozzi, L. Barbieri, C. Leonelli, Incinerator bottom ash and ladle slag for geopolymers preparation, Waste and Biomass Valorization 5 (2014) 393-401

[37] R. Redden, N. Neithalath, Microstructure, strength, and moisture stability of alkali activated glass powder-based binders, Cem Concr Comp, 45 (2014), pp. 46–56

[38] C. Bilim, C.D. Atis, Alkali activation of mortars containing different replacement levels of ground granulated blast furnace slag, Construction and Building Materials 28 (2012) 708–712

[39] M.C. Bignozzi, O. Fusco, A. Fregni, L. Guardigli, R. Gulli, Ceramic waste as new precursors for geopolymerization, Advances in Science and Technology 92 (2014) 26-31

[40] S.P. Wu., J.Q. Zhu, J.J. Zhong, M.D. Wang, Experimental investigation on related properties of asphalt mastic containing recycled red brick powder, Construction and Building Materials 25 (2011) 2883–2887

[41] J. Yang, Q. Du, Y.W. Bao, Concrete with recycled concrete aggregate and crushed clay bricks, Construction and Building Materials 25 (2011) 1935-1945

[42] M. Heikal, K.M. Zohdy, M. Abdelkreem, Mechanical, microstructure and rheological characteristics of high performance self-compacting cement pastes and concrete containing ground clay bricks, Construction and Building Materials 38 (2013) 101–109

[43] C. Poon, D. Chan, Paving blocks made with recycled concrete aggregate and crushed clay brick, Construction and Building Materials 20 (2006) 569-577

[44] M. O'Farrell, S. Wild, B.B. Sabir, Pore size distribution and compressive strength of waste clay brick mortar, Cement and Concrete Composites 23 (2001) 81–91

[45] A. Naceri, M.C. Hamina, Use of waste brick as a partial replacement of cement in mortar, Waste Manage 29 (2009) 2378–2384

[46] A. Moropoulou, A.S. Cakmak, G. Biscontin, A. Bakolas, E. Zendri, Advanced Byzantine cement based composites resisting earthquake stresses: The crushed brick/lime mortars of Justinian's Hagia Sophia, Construction and Building Materials 16 (2002) 543-552

[47] A. Buchwald, C. Kaps, M. Hohmann, Alkali-activated binders and pozzolan cement binders- Compete binder reaction or two sides of the same story?, In Proceedings XI International Congress of Cement Chemistry (ICC), 2003, 1238-1246

[48] J.M. Khatib, R. Siddique, C. Halliday, S. Khatib, Lime activated fly ash paste in the presence of metakaolin, Procedia Engineering 95 (2014) 415-418

[49] T. Hanzlìcek, M. Steinerovà, P. Straka, et al., Reinforcement of the terracotta sculpture by geopolymer composite, Materials and Design 30 (2009) 3229-3234

[50] S. Tamburini, M. Favaro, Magro A., et al., Geopolymers as strenghtening materials for Built Heritage, In Boriani M. et al. (Eds) Proceedings of Built Heritage 2013 – Monitoring Conservation Management, Milan (IT) 18-20 November 2013, p. 1304-1311

[51] K. Elert, E. Sebastiàn, I. Valverde, C. Rodriguez-Navarro, Alkaline treatment of clay minerals from the Alhambra Formation: Implications for the conservation of earthen architecture, Applied Clay Science 39 (2008) 122-132

[52] S. Rescic, P. Plescia, P. Cossari, E. Tempesta, et al., Mechano-chemical activation: An ecological safety process in the production of materials to stone conservation, Procedia Engineering 21 (2011) 1061-1071

[53] E. Franzoni, Rising damp removal from historical masonries: A still open challenge, Construction and Building Materials 54 (2014) 123-136

[54] E. Najafi Kani, A. Allahverdi, J.L. Provis, Efflorescence control in geopolymer binders based on natural pozzolan, Cement Concrete Comp 34 (2012) 25-33

[55] EN 1015-19, Methods of test for mortar for masonry, Determination of water vapour permeability of hardened rendering and plastering mortars, 1998

[56] A. Moropoulou, A. Bakolas, Range of applicability limits of physical, chemical and mechanical characteristics deriving from the evaluation of historic mortars, In: G. Biscontin et al (Eds), Compatible materials for the protection of European cultural heritage, 1998, 165-178

[57] European Standard EN 998-1, Specification for mortar for masonry - Part 1: Rendering and plastering mortar, 2010

[58] L. Binda, A. Saisi, C. Tiraboschi, Investigation procedures for the diagnosis of historic masonries, Constr Build Mater 14 (2000) 199-233

[59] P. Faria Rodriguez, F.M.A.Henriques, Current mortars in conservation: an overview, IntrJrnlRestor 6 (2004) 609-622

[60] M.J.Mosqueraa, B. Silvab, B. Prietob, E. Ruiz-Herreraa, Addition of cement to lime-based mortars: Effect on pore structure and vapor transport, CemConcr Res 36 (2006) 1635-1642

[61] J. Lanas, R. Sirera R., J.I. Alvarez, Study of the mechanical behavior of masonry repair lime-based mortars cured and exposed under different conditions, CemConcr Res 36 (2006) 961–970

[62] L.B.Sickels, Organics vs. Synthetics: Their Use as Additives in Mortars, Symposium Proceedings on Mortars, Cements and Grouts used in the Conservation of Historic Buildings, ICCROM, Rome, Italy (1981) 25-52

[63] H. Vikan, H. Justnes, Influence of vegetable oils on durability and pore structure of mortars, ACI (2006) 417–430
[64] E. Cechová, I. Papayianni, M. Stefanidou, Properties of lime-based restoration mortars modified by the addition of linseed oil, in 2nd Historic Mortars Conf. RILEM, Praugue, 2010 pp. 937–945

[65] E. Cechová, The effect of linseed oil on the properties of lime-based restoration mortars, Doctoral dissertation in Alma Mater Studiorum Università di Bologna (2009), DOI 10.6092/unibo/amsdottorato/2267

[66] M. Stefanidou, A. Karozou, M. Kapsimani "Protecting adobes by increasing their hydrophobicity using alternative methods" 5th INTERNATIONAL CONFERENCE, YOCOCU 2016, 21st-23rd September 2016, Madrid, Spain

[67] C. Nunes, Z. Slížková, Hydrophobic lime based mortars with linseed oil: Characterization and durability assessment, CemConcr Res 61-62 (2014) 28-39

[68] S. Fang, B. Zhang, G. Li, A study of Tung oil lime putty: A traditional lime based mortar, Int J AdhnAdhv 48 (2014) 224–230

[69] C. Nunes, Z. Slížková, Freezing and thawing resistance of aerial lime mortar with metakaolin and a traditional water-repellent admixture, Constr Build Mater 114 (2016) 896-905

[70] A. Lagazzo, S. Vicini, C. Cattaneo, R. Botter, Effect of fatty acid soap on microstructure of lime-cement mortar, Constr Build Mater 116 (2016) 384–390

[71] N. Van Tuan, G. Ye, K. Breugel, A.L.A Fraaij, D. Bui, The study of using rice husk ash to produce ultra high performance concrete, Constr Build Mater 25 (2011) 2030-2035

[72] K. Callebaut, J. Elsen, K. Balen, W. Van Viaene, Nineteenth century hydraulic restoration mortars in the Saint Michael’s Church (Leuven, Belgium) Natural hydraulic lime or cement?,CemConcr Res 31 (2001) 397–403

[73] E. Zendri, V. Lucchini, G. Biscontin, Z.M. Morabito, Interaction between clay and lime in “cocciopesto” mortars: a study by 29 Si MAS spectroscopy, Appl Clay Sci 25 (2004) 1–7

[74] G. Matias, P. Faria, I. Torres, Lime mortars with heat treated clays and ceramic waste: A review. Constr Build Mater 73 (2014) 125-136

[75] S. Donatello, M. Tyrer, C.R. Cheeseman, Comparison of test methods to assess pozzolanic activity, CemConcr Comp 32 (2010) 121–7

[76] P. Cachim, A. Velosa A., F. Rocha, Effect of Portuguese metakaolin on hydraulic lime concrete using different curing conditions, Constr Build Mater 24 (2010) 71–78

[77] J. Jasiczak, K. ZielinskiEffect, Effect of protein additive on properties of mortar, Cem. Concr. Compos 28 (2006) 451–457

[78] C. Arcolao , Le ricette del restauro:malte, intonaci, stucchi dal 15 al 19 secolo, Marsilio, Venice, 1998

[79] E. Alonso, L. Martinez-Gomez, W. Martinez, V.M. Castano, Preparation and characterisation of ancient-like masonry mortars, Adv. Compos. Lett., 11 (2002) 33–36

[80] S.Q. Fang, H. Zhang, B.J. Zhang, Y. Zheng, The identification of organic additives in traditional lime mortar, J. Cult. Herit., 15 (2014) 144–150

[81] H.Y. Rao, B. Li, Y.M. Yang, Q.L. Ma, C.S. Wang, Proteomic identification of organic additives in the mortars of ancient Chinese wooden buildings, Anal. Methods, 7 (2015) 143–149

[82] EN 459-1:2010. Building lime. Part 1: Definitions, specifications and conformity criteria, 2010

[83] EN 196-1, Testing method for determining the strength of cement, Determination of mechanical resistance, 2005

[84] Circular of the Italian Ministry of Health, n 1 of January 1991: Oils and fats used for frying (CM 1991, No.2568/91)

[85] EN 1015-2, Methods of test for mortar for masonry Part 3: Determination of consistency of Fresh Mortar, 1999

[86] EN 1015-18, Methods of test for mortar for masonry: Determination of water absorption coefficient due to capillary action of hardened mortar, 2004

[87] EN 15802, Conservation of cultural property. Test methods, Determination of static contact angle, 2010

[88] G. Groot, J. Ashall, J.J. Hughes, Characterisation of old mortars with respect to their repair, RILEM TC 67-COM, Springer, New York (2004) 77–106

[89] D. Kivánková, C. Nunes, Z. Slížková, D. Frankeová, K. Niedoba, High-performance repair mortars for application in severe weathering environments: frost resistance assessment, Proc. 3rd Historic Mortars Conference, Glasgow, 2013.

[90] E. Wendler, A.E. Charola, Water and its interaction with porous inorganic building materials, Proc. Hydrophobe V: 5th Int. Conf. on Water Repellent Treatment of Building Materials, Aedificatio Publishers (2008) 57–74

[91] M. Lazzari, O. Chiantore, Drying and oxidative degradation of linseed oil, Polym. Degrad. Stab. 65 (2) (1999) 303–313

[92] C. Alberioa, N.G. Izquierdoa, T. Galellac, S. Zuild, R. Reidc, A. Zambellic, L.A.N. Aguirrezábala, A new sunflower high oleic mutation confers stable oil grain fatty acid composition across environments, Eur J Agron 73 (2016), pp. 25–33

[93] T. Togkalidou, M. Karoglou, A. Bakolas, A. Giakoumaki, A. Moropoulou, Correlation of water vapor permeability with microstructure characteristics of building materials using robust chemometrics, Transp Porous Med 99 (2013) 273-295

[94] V. Corinaldesi, Environmentally-friendly bedding mortars for repair of historical buildings,Constr Build Mater 35 (2012) 778–784

[95] S. Andrejkovicováa, A.L. Velosab, E. Ferrazb, F. Rochaa, Influence of clay minerals addition on mechanical properties of air lime–metakaolin mortars, Constr Build Mater 65 (2014) 132–139

[96] C. Lutchman, D. Evans, W. Al Hashemi, R. Maharaj, 7 Fundamentals of an operationally excellent management system, CRC Press, Google books. Web. 23 Oct. 2015. pp. 397, http://books.google.com

[97] E. Vejmelková, M. Keppert,Z. Keršner, P. Rovnaníková, R. Cerný, Mechanical, fracture-mechanical, hydric, thermal, and durability properties of lime-metakaolin plasters for renovation of historical buildings,Constr Build Mater 31 (2012) 22–28

[98] E. Vejmelková, D. Konáková, M. Cáchová, M. Keppert, R. Cerný, Effect of hydrophobization on the properties of lime–metakaolin plasters, Constr Build Mater 37 (2012) 556–561

[99] Putting Tensiometry to Work (2015, June 23). Retrieved from http://www.biolinscientific.com/attension/applications/?card=AA7

[100] Klein N.S., Bachmann J., A. Aguado, Toralles-Carbonari B., Evaluation of the wettability of mortar component granular materials through contact angle measurements, Cem Concr Res 42 (2012) 1611–1620

[101] A. Izaguirre, J. Lanas, J.I. Alvarez,Effect of water-repellent admixtures on the behaviour of aerial lime-based mortars, CemConcr Res 39 (2009) 1095–1104

[102] M.J. Mosquera, D. Benitez, S.H. Perry, Pore structure in mortars applied on restoration: Effect on properties relevant to decay of granite buildings, CemConcr Res 32 (2002) 1883-1888

[103] ASTM C 191, Standard test methods for time of setting of hydraulic cement by Vicat needle, 2008

[104] UNI 10859, Cultural Heritage - Natural And Artificial Stones - Determination Of Water Absorption By Capillarity (2000)

[105] UNI 11432, Cultural Heritage - Natural and Artificial Stone - Determination of the Water Absorption by Contact Sponge (2011)

[106] RA. Latour, Biomaterials: protein–surface interactions, Wnek GE, Bowlin GL, editors, The Encyclopedia of Biomaterials and Bioengineering

APPENDICES

Appendix A

Schematic illustration of the binders synthesis - Phase 1

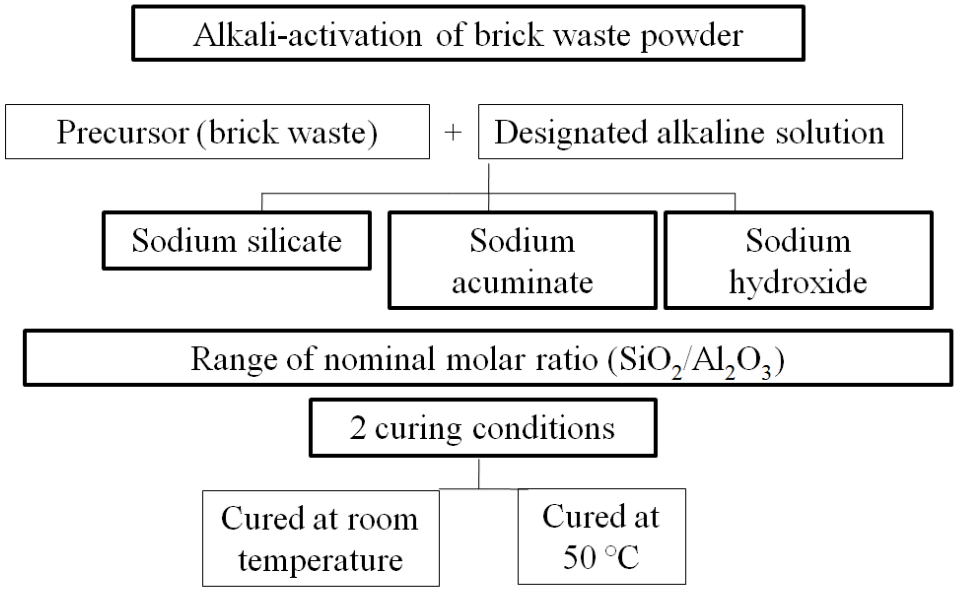

Appendix B

Schematic illustration of the mortars synthesis - Phase 2

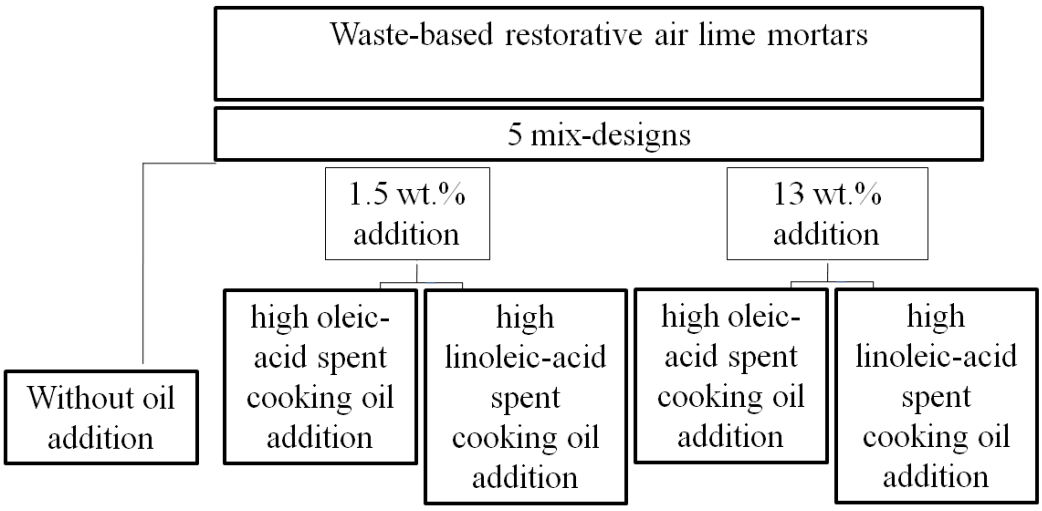

Appendix C

Schematic illustration of the mortars synthesis - Phase 3

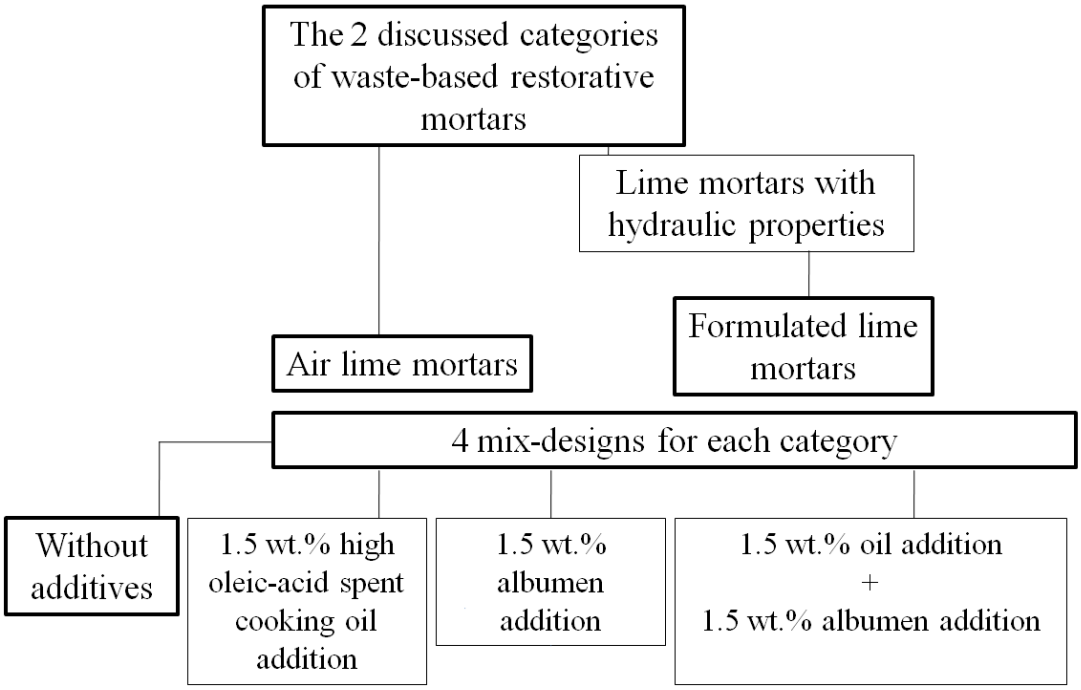

ACKNOWLEDGMENTS

Firstly, I would like to thank my supervisor, prof. Dr. Maria Chiara Bignozzi, for giving me the chance to be her first international PhD candidate. She supervised and leaded my research in a flawless way and provided an opportunity for me to scientifically grow up in her group. I am really thankful of her for all supports during these three years. The freedom of thought and action I enjoyed in her group is greatly acknowledged.

I sincerely thank Dr. Stefania Manzi for being always present and helpful and for her kind and professional co-supervision.

I especially thank Dr. Sansonetti for giving me the valuable opportunity of using his knowledge and experiences in CNR-ICVBC of Milan, for considering me worthy of continuing and for his efforts to make it happen.

I am also thankful for the three years of fellowship and hospitality I received in the Institute of Advanced Studies of University of Bologna. Special thanks are due to Dr. Barbara Cimatti for all her supports. I learned a lot as the referent of ISA junior fellows during 2014-2016.

I thank Dr. Elisa Franzoni, and my humble friend Dr. Enrico Sassoni, for scientific supports and precious comments and discussions.

I am grateful to Dr. Giovanni Pascale and Dr. Elisabetta Rosina, for their priceless suggestions that directed me in finding the right place for such a PhD project.

I thank my colleagues Dr. Maria Elia Natali, Dr. Gabriela Graziani, eng. Giulia Masi, eng. Lorenza Carabba, and eng. Serena Andreotti for creation of a pleasant and friendly work environment. I kindly thank the lab technician of LASTM, Mr. Paolo Carta, for his help and availability.

I would like to thank my parents for their unconditional support and love, and to my kind sister-in-law, Laleh. Finally, grateful acknowledgment is due to my brother, Pooria; the support he has provided me over the years was the greatest gift.